COLLEGE OF WILLIAM AND MARY PHYSICS DEPARTMENT

Mechanical Properties of Polymer Nanocomposites Based on Functionalized Graphene Sheets

By Thomas J. Wallin

Advisor Hannes Schniepp

5/5/2010

A report submitted in partial fulfillment of the requirements for a degree in Physics from the College of William and Mary in Virginia.

Abstract

Recent preliminary research on functionalized graphene sheets (FGS) has shown this material to be a model candidate for use in making nanocomposites with impressive mechanical properties. The objective of this work is to create a method for adding and uniformly dispersing FGS to polymers and measure the mechanical properties of these FGS loaded nanocomposites and compare to those of the neat polymer systems. The effect that the addition of FGS has on the glass transition temperature(T_g) was also observed. From this comparison, we hope to find a polymer system in which an addition of some low weight percentage of FGS improves all of the following: tensile modulus, strain at break, ultimate strength and thermal resistance. Three polymers polymethyl methacrylate (PMMA), polyvinylalcohol (PVA), and polyetherimide (PEI) were examined from this perspective. The previously measured nanoparticle-polymer interfacial interaction between FGS and these three polymers allows for a fundamental understanding of the results.

List of Figures

Figure 1: Contact Mode AFM Scan of a Single Graphene Sheet 2
Figure 2: Stress Strain Curves for Neat PVA 10
Figure 3: Stress Strain Curve for 0.05% FGS2 in PVA 11
Figure 4: Stress Strain Curve for 0.1% FGS2 in PVA 12
Figure 5: Sample TGA for PVA 14
Figure 6: Modulus vs. Solvent Content for Neat PVA 15
Figure 7: Elongation at Break vs. Solvent Content for Neat PVA 16
Figure 8: Stress Strain Curves for Neat PMMA 18
Figure 9: Stress Strain Curves for 0.01% FGS2 in PMMA 19
Figure 10: Stress Strain Curves for 0.1% FGS2 in PMMA 20
Figure 11: Sample TGA for PMMA 21
Figure 12: Modulus vs. Solvent Content for Neat PMMA 23
Figure 13: Elongation at Break vs. Solvent Content for Neat PMMA 24
Figure 14: Stress at Break vs. Solvent Content for Neat PMMA 24
Figure 15: Stress Strain Curves for Neat PEI 26
Figure 16: Stress Strain Curves for 0.05% FGS2 in PEI 27
Figure 17: Stress Strain Curves for 0.1% FGS2 in PEI 28
Figure 18: Sample TGA for PEI 30
Figure 19: Neat PVA Glass Transition Temperature Measurement by DSC 31
Figure 20: 1.0% FGS2 in PVA Glass Transition Temperature Measurements by DSC 32
Figure 21: Neat PMMA Glass Transition Temperature Measurement by DSC 33
Figure 22: 0.2% FGS2 in PMMA Glass Transition Temperature Measurement by DSC 34
Figure 23: Neat PEI Glass Transition Temperature Measurement by DSC 35
Figure 24: 0.1% FGS2 in PEI Glass Transition Temperature Measurement by DSC 36

List of Tables

Table 2: Summary of PVA Results 13
Table 3: Effect of Solvent Content on Tensile Measurements for PVA 15
Table 4: PVA Comparison of Tensile Properties with Interpolated Equal Solvent Content 17
Table 5: Summary of PMMA Results 22
Table 6: Effect of Solvent Content on Tensile Measurements for PMMA 23
Table 7: PMMA Comparison of Tensile Properties with Interpolated Equal Solvent Content 25
Table 8: Summary of PEI Results 29
Table 9: Summary of Glass Transition Temperature Results 36

Table of Contents

Introduction 1
Experimental 5
Preparation of Polymer Films 5
Mechanical Testing 6
Solvent Characterization 8
Thermal Resistance 9
Results 10
Mechanical Testing Results for PVA 10
Mechanical Testing Results for PMMA 18
Mechanical Testing Results for PEI 26
Glass Transition Temperature Results 30
Discussion 37
Acknowledgements 41
References 42

Introduction

Composites have the potential to take two materials and combine them in a way that results in a material with superior properties to those of its constituents. The structural advantages of such materials are used frequently, an example being the use of metal rebar in concrete. Nanocomposites, as the name implies, are materials in which particles, of a dimension less than 100 nm[1], have been added into a polymer matrix. Ideally, polymer nanocomposites will exhibit the best properties of its components, allowing for exciting new combinations of properties and consequently material applications.[1,2] Though the particles are on the nanoscale, the large surface area of the particles create strong particle-polymer interactions at low nanoparticle additions.[3] Thus, without the need to add large amounts of particles to attain these strong interactions, cheap, high performance, lightweight materials are possible.[4,-7] The practical applications of nanocomposites has obvious potential benefits for structural materials, such as lighter, more fuel efficient transportation vehicles.[8-11]

The obvious advantages of nanocomposites are not currently realized because of the lack of a controlled, large scale processing method.[1] For example, it is challenging to exfoliate and disperse the nanoparticle as necessary to ensure the large surface area required for the strong polymer-particle interaction.[12,13] Moreover, the current nanoparticles are expensive and difficult to produce in macroscopic amounts (Carbon nanotubes can cost over $100,000/kg). Lastly, a current lack of understanding limits the ability to predict the optimal production method.[14,15] Functionalized graphene sheets (FGS) offer the potential solutions to these processing problems.

Idealized graphene is a network of just carbon atoms, like graphite. Graphene is a single layer, or sheet, of sp^2 hybridized carbons. Whereas graphite is multiple layers of graphene stacked upon each other. The carbons in graphene exist in a “honeycomb” network of repeating six membered rings. This same honeycomb network of carbon is seen in carbon nanotubes, a nanofiller used for its extreme

strength. Therefore we can expect single layered graphene to have a strength similar to single walled carbon nanotubes[2,3,5]. Recently[7,12,16,17], graphene has been produced by exfoliating graphite. More generally, exfoliation means that we can separate the layers of graphene, that make up graphite, from each other. This creates graphene sheets with a thickness of only one atom. Atomic force microscopy found the other diameter of the sheets to be on the order of 100 nm. The huge difference in the thickness and diameter allows for the large surface to volume ratio desired for nanoparticles.

Recent work has managed to economically produce large amounts of exfoliated graphene with varying degrees of functionalization cheap and common graphite ($5/kg).[7,16-21] In our study, we employed harsh acids such to exfoliate the graphite. As a side effect, the graphene is functionalized. This nomenclature refers to the fact that the acids also oxidize graphite by adding oxygen based functional groups (such as hydroxyl and epoxide)[12]. The graphite oxide (GO)-acid slurry is then filtered using a Buchner funnel and deionized water until the filtrate is of a neutral pH. The GO is then dried and forms and stored as "GO" flakes. Next, these GO flakes are sonicated to exfoliate and disperse individual functionalized graphene sheets into a solvent. Below is an image taken by AFM of the FGS sheets.

Figure 1: Contact Mode AFM Scan of a Single Graphene Sheet

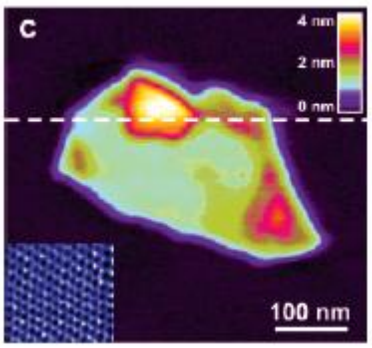

Since the polarity of FGS can be attributed to the presence of the functional groups, we can adjust the polarity by adjusting the functionalization. By changing the polarity of the sheets, we can achieve dispersion in a wide range of solvents.[22,23] The ability to disperse FGS in a wide variety of solvents allows this nanoparticle to be potentially added to an equally wide range of polymers. Lastly, the use of atomic force microscopy a method for quantitatively characterizing the interfacial interaction between FGS and multiple polymers has been developed, which may eventually allow for a better understanding of the nanocomposite's potential.[23,24] In our studies, FGS-2, meaning functionalized graphene sheets with a carbon to oxygen ratio of 2:1, serves as our nanofiller particle.

We wish to find a system of known composition in which all the measured mechanical properties are improved at relatively low weight compositions of FGS. As part of this goal, we will need to create a method for adding varying amounts of FGS sheet nanoparticles into a variety of polymers in a method that yields a suitable polymer film.

We study the tensile modulus, strain, and ultimate strength using a mechanical testing system. Since solvent content can drastically affect the mechanical properties of a polymer[25] by changing the particle interactions, we minimize and quantify the solvent content in all of our polymers during preparation. Ultimately, we desire zero solvent concentration in order to accurately quantify the polymer-particle interactions. We study the glass transition temperature relative to the neat polymer because this is a measure of thermal stability, an important consideration for application of the nanocomposite.[2,26] Relatively low weight concentrations of functionalized graphene sheets have been noted to have unprecedented and rather large shifts in glass transition temperature of polymers.[2] Differential scanning calorimetry (DSC) was employed for glass transition measurements.

Polymethyl methacrylate (PMMA) was one polymer chosen to study. It is a clear thermoplastic. PMMA is also a commonly used, well understood polymer. PMMA can dissolve in many solvents,

including dimethylformamide (DMF). Experimentally, PMMA is very stiff and brittle with a modulus of around 2.1GPa[2]. The FGS then has the potential to drastically improve the mechanical properties of this system.

The second polymer we chose to characterize and measure the properties of the polyvinyl alcohol (PVA) polymer system. PVA is a clear, high tensile strength, resistant to non-polar solvents and water soluble. It has already been demonstrated in this laboratory that FGS2 can be dispersed in water. The potential to add FGS2 to a system of water without the use of organic solvents is environmentally and economically attractive.

Lastly, we studied polyetherimide (PEI). PEI is a transparent-yellow amorphous thermoplastic often used in applications for its thermal stability. Commonly known as Ultem, PEI has markedly different properties than PMMA. PEI is less brittle, has a higher glass transition temperature, and more solvent resistant, as DMF will not dissolve this polymer. However, one solvent that does dissolve PEI is dimethylacetamide (DMAc). DMAc can not maintain a dispersion of FGS2. We wish to attempt to overcome this solvent problem by capitalizing on the fact that DMAc and DMF are miscible. A FGS2/DMF dispersion will be added to a solution of PEI/DMAc. The success of this method to maintain an FGS2 dispersion will offer a way to overcome solvent compatibility problems in other problems.

The interfacial interaction strength between FGS-2 and multiple polymers have been qualitatively characterized in this laboratory using Atomic Force Microscopy.[23] FGS-2 was spun on a substrate. A polymer was then placed on top of the FGS2 and peeled off of the substrate. The surfaces of the substrate and polymer are then studied to determine the location of the FGS sheets, it is assumed the surface with the strongest interaction, the substrate or the polymer, will show the presence of FGS2. By varying the polymer and the substrate, we can rank polymers in order of their interaction strength. All three polymers in this study were analyzed from this perspective and the interaction strength from

weakest to strongest of these three polymers and FGS-2 was found to be PEI<PMMA<PVA.[23] With this information in mind, we can note any trends in the mechanical properties and strength of nanoparticle-polymer matrix interaction with our chosen polymers to further develop the understanding of nanocomposites.

Experimental

Preparation of Polymer Films

There was no established method for preparing FGS-2 loaded composites for these polymers. Our general method is to dissolve the polymer pellets into a solvent, add dispersed FGS in a solvent (not necessarily the same as the polymer solvent) and then drive off all solvent until you have only polymer and nanoparticle. The PMMA composites were prepared from Aldrich pellets (average M_w 120,000) and the solvent dimethylformamide (DMF). The PEI was prepared from Ultem pellets given to Professor Kiefer from NASA and dimethyl acetamide (DMAc) served as the solvent. PVA was prepared from Aldrich (average M_w 31,000) flakes using deionized water as the solvent. In each case, enough solvent was added to completely dissolve the polymer pellets into a solution of known polymer mass concentrations were made. Knowing the original mass of the polymer pellets and using a prepared solution of either 1 mg /1 mL of FGS-2/DMF mixture (PMMA and PEI polymers) or 1mg/mL of FGS-2/water mixture (PVA polymers only), we added our desired amount of FGS-2 and attain our desired composite composition. The polymer-solvent-FGS solution was stirred and heated (around 60˚C) for a few hours before being poured.

The solvent-polymer solutions are then cast on a flat, level surface. The polymer film should be able to be easily lifted from the surface so as to not strain or damage the film before testing. Glass sheets were used for PEI and PVA. It was found that PMMA is not easily removed from glass sheets so Teflon sheets were used for that system. Next, we wish to remove as much solvent as possible from the

polymer-solvent film. We desire films that are level, smooth and without bubbles as these imperfections may cause the sample to fail prematurely during mechanical testing. Removing the solvent too quickly can cause air bubbles and concentration gradients to form in the material. It was found that PMMA and PVA dry best over a 4 day treatment in a dry-box, while PEI is best dried in a 90 ˚C oven over a period of 4 days. It was found that covering the sample with a paper towel or glass plate about a half an inch above the film prevented air flow from disturbing the surface.

Mechanical Testing

In order to test the composites mechanically, we first have to prepare suitable samples from the films. We wish to analyze the Young's modulus, elongation and tensile strength for each composite using a MTS 810 Material Test System. This kind of measurement requires samples be of a "dog bone" shape. We cut the composite into this shape by placing a small dog bone shaped blade (Dewes Gumbs Die Co. Inc. DGD Expulsion Press ASTM Test Dies) on top of the film and punching the blade through the film using a Carver Laboratory Press. Complications did arise, in particular with the brittle PMMA system as the press cracked many dog bones during punching. Through trial and error it was discovered that heating the dog bone blade to 120 ˚C would allow for cleaner, smoother dog bones to be punched from the film.

Once suitable dog bone samples are made, tensile measurements can be conducted. During later calculations, we will need to know the cross sectional area of the sample so initial dimension measurements (length, thickness and width) are made using a caliper. Then we will use hydraulic wedge grips to secure both ends of the dog bone. Then the material testing system will experimentally apply a increasing load in order to maintain a rate of stretching of 0.25 inches per minute. The stretching continues until the sample breaks, making this a destructive measurement. During this process, a computer periodically measures the stroke (or distance the sample has stretched), and the force (load)

on the sample. From this data we can calculate the percent elongation (strain), stress on the sample and Young's modulus.

First, we wish to calculate the percent elongation or strain (ε) the sample has experienced. This is found by comparing the stroke (length the dog bone has stretched) to the measured length before the trial.

$$Elongation = \varepsilon = \frac{Stroke + Initial\ Length}{Initial\ Length} \quad (1)$$

Next, we want to calculate the stress or force per unit area on the sample. In order to do this, we need to know the cross sectional area of the sample, which is constantly changing with strain. We calculate the cross sectional area of the dog bone by using the initial volume, initial length, and increase in the length of the dog bone at that time (stroke). Since volume is constant, this new area is the initial volume divided by the sum of the stroke and initial length.

$$New\ Cross\ Sectional\ Area = \frac{Initial\ Volume}{Stroke + Initial\ Length} \quad (2)$$

The stress is then simply the measured force divided by the new cross sectional area at that time. We calculate the stress and strain for each set of measured force and stroke values from the material testing system.

The tensile modulus (E) is defined by equation 3.

$$E = \frac{\sigma}{\varepsilon} = \frac{F/A}{\Delta L/L} \quad (3)$$

Where σ is the stress (force divided by cross sectional area), ε is strain (given by the percent elongation. To calculate the tensile modulus, we will plot the all of the calculated stress values on the y-axis and the corresponding strain values on the x-axis. The slope will be the modulus. This plot is not

entirely linear. This deviation from linearity occurs because the modulus is not constant, but can be a function of the stroke. Stress-hardening, necking and tearing can all cause the modulus to change during the trial. However, the data at the beginning of the measurement (or when the strain is close to zero) is linear and the slope from this initial region is taken as the modulus.

When the sample breaks, the stress and modulus drop to zero. The first strain value that corresponds to this zero stress is the elongation at break. The load at break is taken as the local maximum in strain value before sample destruction. Since the modulus, tensile stength and elongation at break are all found to be dependent on solvent composition, a piece of each of the destroyed mechanical testing samples is then used for solvent characterization measurements.

Solvent Characterization

Thermogravimetric Analysis (TGA) is the process by which we characterized our solvent content. A piece of each film (or destroyed dog bone), weighing about 15 mg, is broken off and that sample is carefully weighed while being subjected to a heat treatment in an inert (N_2) environment. The change in weight can be followed as the temperature varies and will allow us to determine the mass loss and identify what species is being driven off of the sample. From this we can calculate the weight percent of the solvents in the film. The net heat treatment for each sample was determined by the melting points of the polymer and the boiling points of the solvents. However, for each polymer system, the same heat treatment was applied to ensure reproducibility. The treatment for PMMA involved a temperature hold at 110˚C for water removal, and a temperature hold again at 160˚C for DMF removal. PEI was also held at 110˚C for water removal, but then held at a higher temperature of 250˚C for DMF and DMAc removal. PVA needed only water removal and as such was held at 110˚C.

The resulting information was compiled and combined into a plot of weight percent versus time and temperature versus time. From a comparison of these graphs, we can integrate all the solvent

evaporated at each temperature hold, and thereby measure the solvent content. A sample TGA plot for is shown for each polymer in figures 4,10, and 17.

Thermal Resistance

The thermal resistance measurements were done by finding the glass transition temperature. Differential scanning calorimetry (DSC) was employed in this measurement. DSC uses a heating resistor to vary the temperature of the sample in a aluminum pan and simultaneously measures the power input (P = IR), and consequently heat flow, necessary for this temperature change. Simultaneous measurements are made on an empty pan. By subtracting the heat flow and temperature change in the empty pan we can get a measure of the heat flow into just the sample. Using the sample's previously measured mass, we can easily calculate the heat capacity. During the transition from the glassy to rubber state, the heat capacity appears to "step." Thus an inflection in the plot of heat flow versus temperature will correspond to the temperature of the glass transition. We will cycle the temperature above and below the glass transition a few times until the observed values for T_g agree. One benefit of this method is that the temperature ramp drives off the solvent, minimizing possible unwanted solvent contributions. We again want to make sure that we avoid too harsh a heat treatment, as we might reduce the functionalized graphene sheets or cause degradation of the polymer. For PEI, we cycled the temperature from 150˚C to 250˚C at a rate of 3˚C/min. For PMMA we varied from 110˚C to 150˚C at 3˚C/min. The PVA method was from 60˚C to 130˚C at 3˚C/min.

Results

Mechanical Testing Results for PVA

The mechanical results for PVA were measured and calculated as described above. The stress strain curves are shown in figures 2,3 and 4. A summary of the results are shown in Table 1.

Figure 2: Stress Strain Curves for Neat PVA

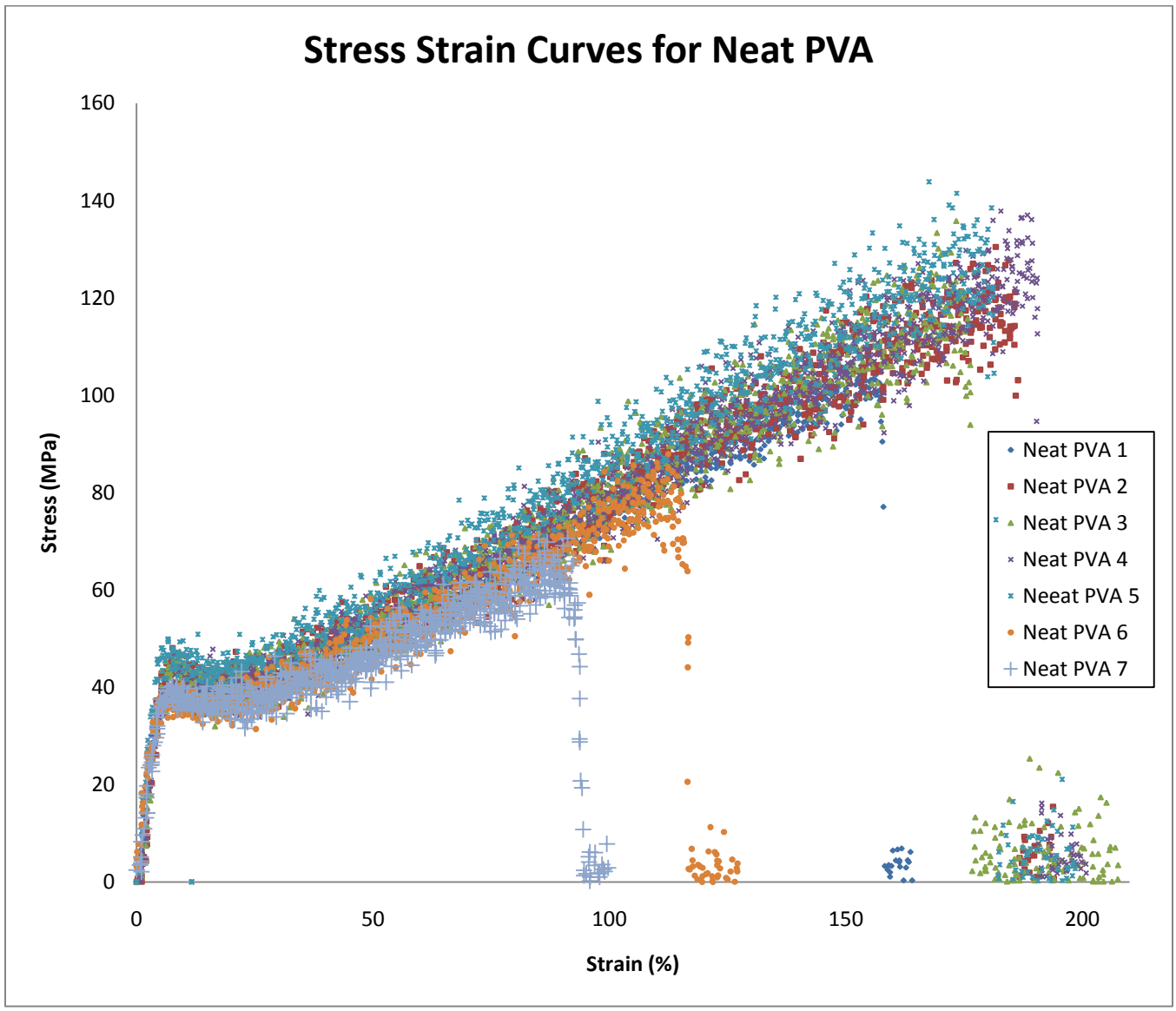

Figure 3: Stress Strain Curve for 0.05% FGS2 in PVA

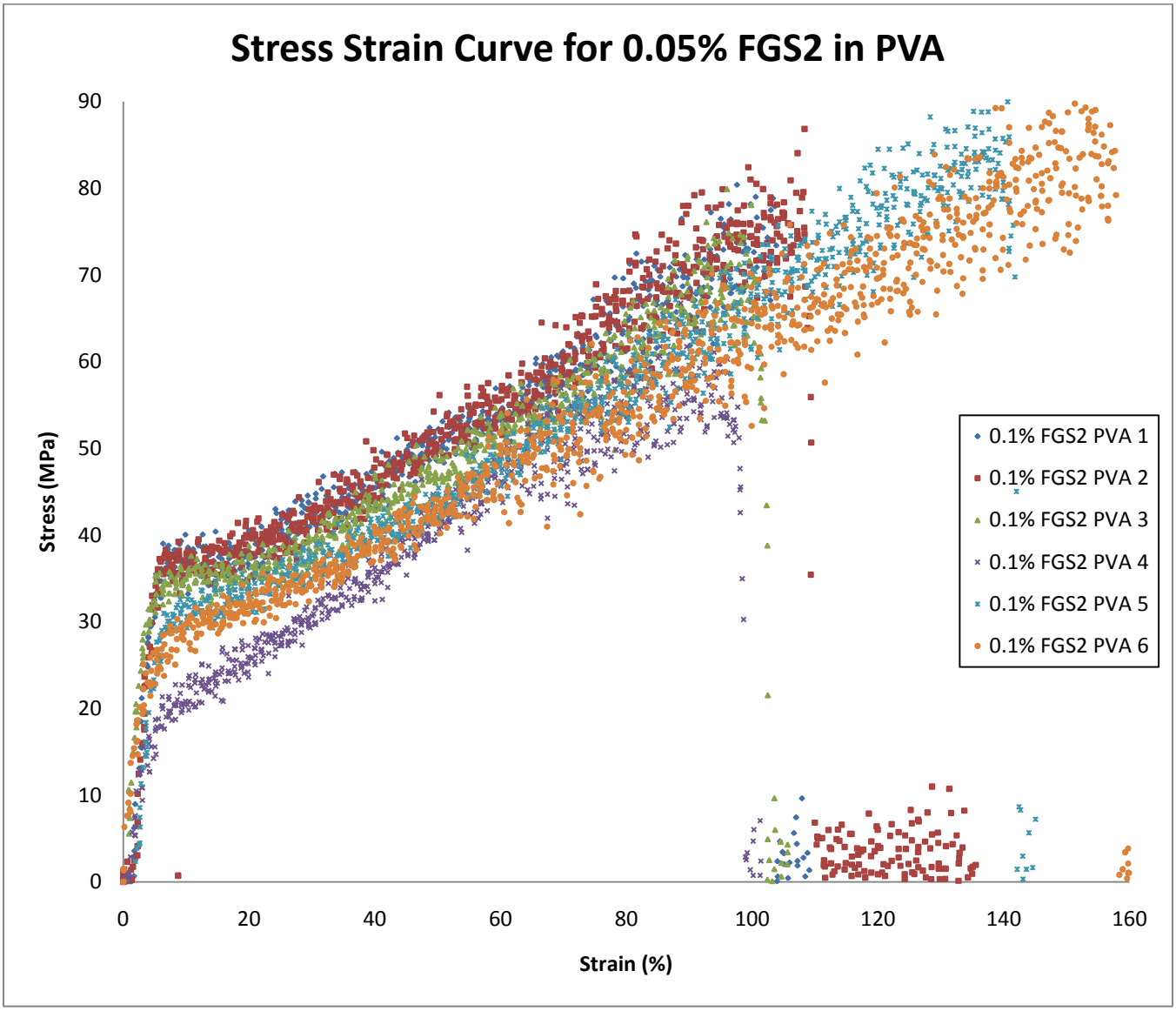

Figure 4: Stress Strain Curve for 0.1% FGS2 in PVA

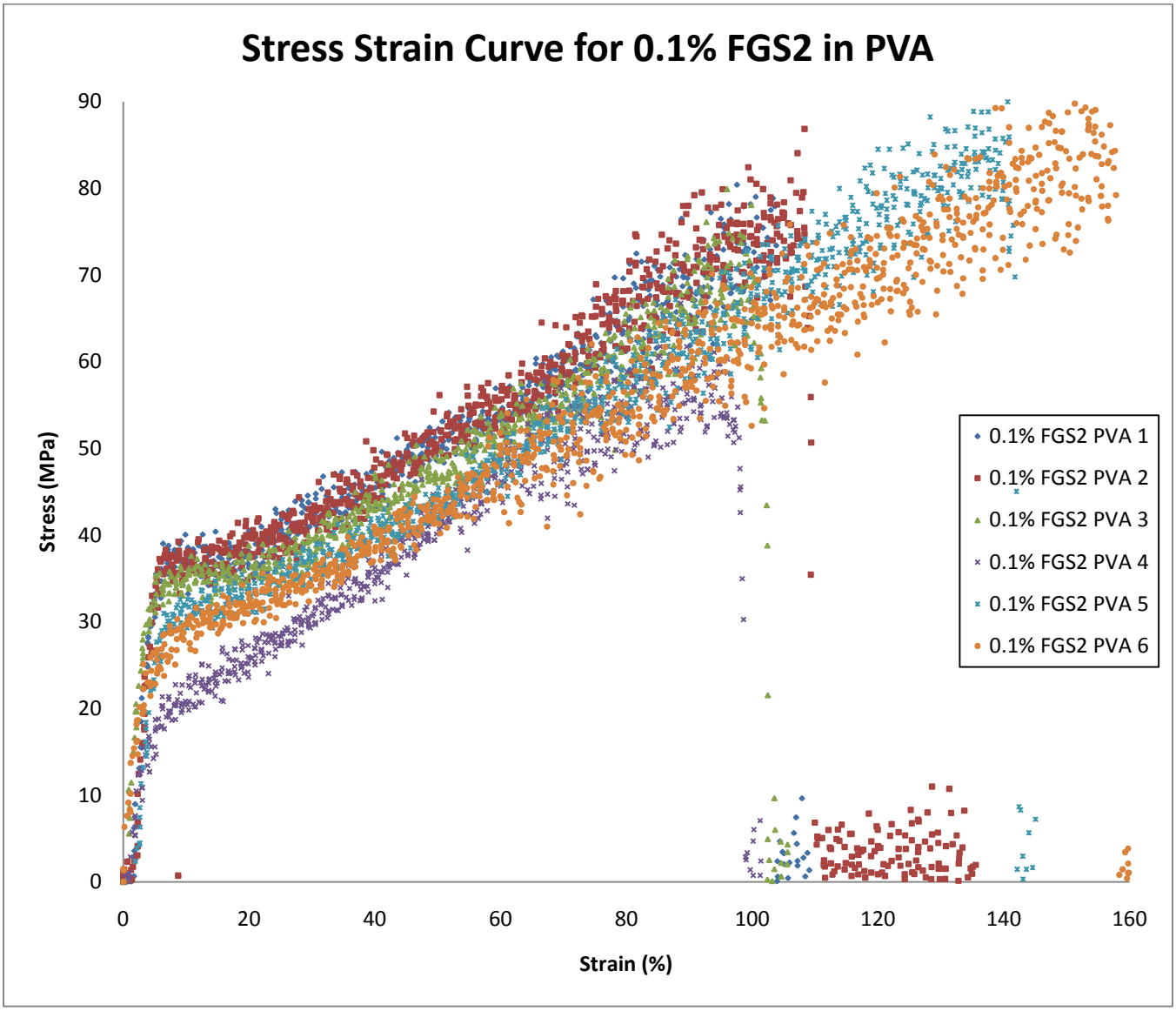

Table 1: Summary of PVA Results

Sample	Modulus (MPa)	Elong. @ brk. (%)	Stress @ brk. (MPa)	Solvent content (Weight %)
Neat 1	950	160	100	6.4
Neat 2	1010	190	120	6.4
Neat 3	1120	180	120	6.4
Neat 4	960	190	130	6.4
Neat 5	1340	180	130	6.4
Avg	**1080**	**180**	**120**	
St. Dev.	**160**	**10**	**10**	
0.5% FGS2 1	170	270	110	6.0
0.5% FGS2 2	540	190	90	6.0
0.5% FGS2 3	610	180	90	6.0
0.5% FGS2 4	630	180	100	6.0
0.5% FGS2 5	580	190	90	6.0
0.5% FGS2 6	500	270	–	6.0
0.5% FGS2 7	670	220	110	6.0
Avg	**590**	**210**	**100**	
St. Dev.	**60**	**40**	**10**	
1.0% FGS2 1	1100	100	70	6.5
1.0% FGS2 2	1030	110	80	6.5
1.0% FGS2 3	1080	100	70	6.5
1.0% FGS2 4	510	100	60	6.5
1.0% FGS2 5	710	140	90	6.5
1.0% FGS2 6	670	160	90	6.5
1.0% FGS2 7	760	190	110	6.5
Avg	**840**	**130**	**80**	
St. Dev.	**230**	**30**	**20**	

This data seems to show that the presence of FGS-2 at these concentrations decreases the modulus. However, most importantly, we see that the solvent concentrate on is not the same for each concentration. We measured the solvent concentration via thermogravimetric analysis. A sample TGA is shown in figure 5.

Figure 5: Sample TGA for PVA

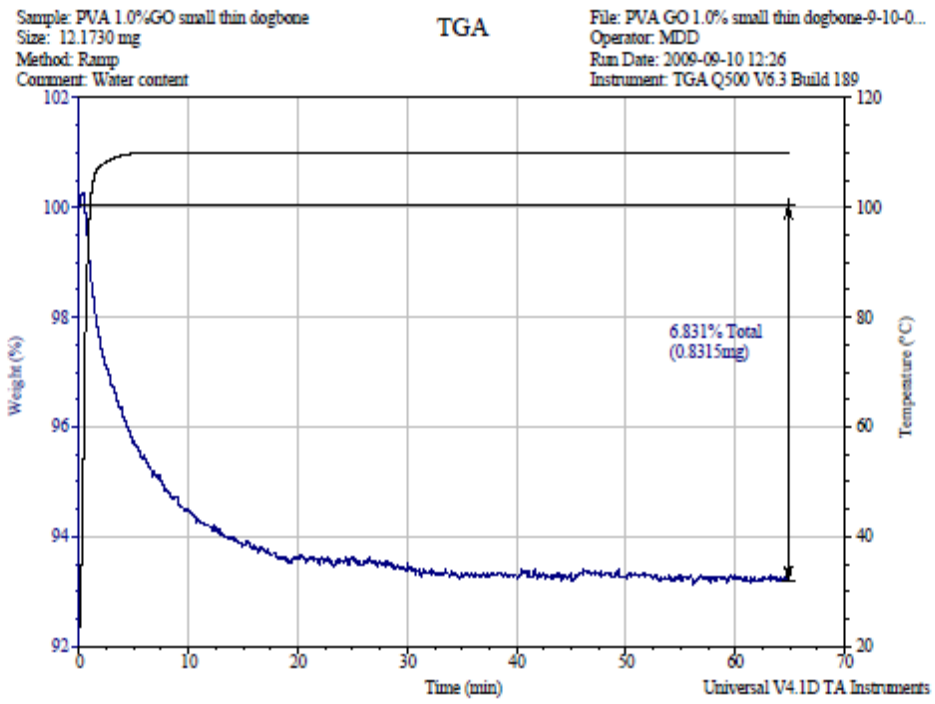

The solid black line is the plot of the temperature as a function of time. The blue line is the weight percentage as a function of time. We note that over the treatment, the temperature is ramped to 110˚C and the mass drops by 6.8% (shown by the arrows). This change in mass is attributed solely to the evaporation of the solvent and is therefore used as the solvent content.

We noted that the measured modulus for the neat PVA sample did not match up with the mechanical data measured for other previous batches of neat PVA (made for another study) with different solvent contents. Using the average calculated modulus, and percent elongation values from the previous PVA studies, we compiled Table 2. The ultimate strength or stress at break was omitted as it was not recorded for the earlier batches.

Table 2: Effect of Solvent Content on Tensile Measurements for PVA

Solvent Content (Weight %)	Modulus (Mpa)	Elongation (%)
5	1300	7
6.4	1080	180
7.5	540	190
10	70	280

Other studies in other polymer nanocomposites (based on clay nanofillers) show that above a minimum solvent and below a maximum solvent content, there exists a region where mechanical properties are proportional to the solvent composition.[25] Looking to see a proportional relationship, we decide to plot the modulus and elongation at break versus the solvent content of PVA (the data shown in Table 2). A linear relationship was noted and best fit plots were constructed and are shown in figures 6 and 7.

Figure 6: Modulus vs. Solvent Content for Neat PVA

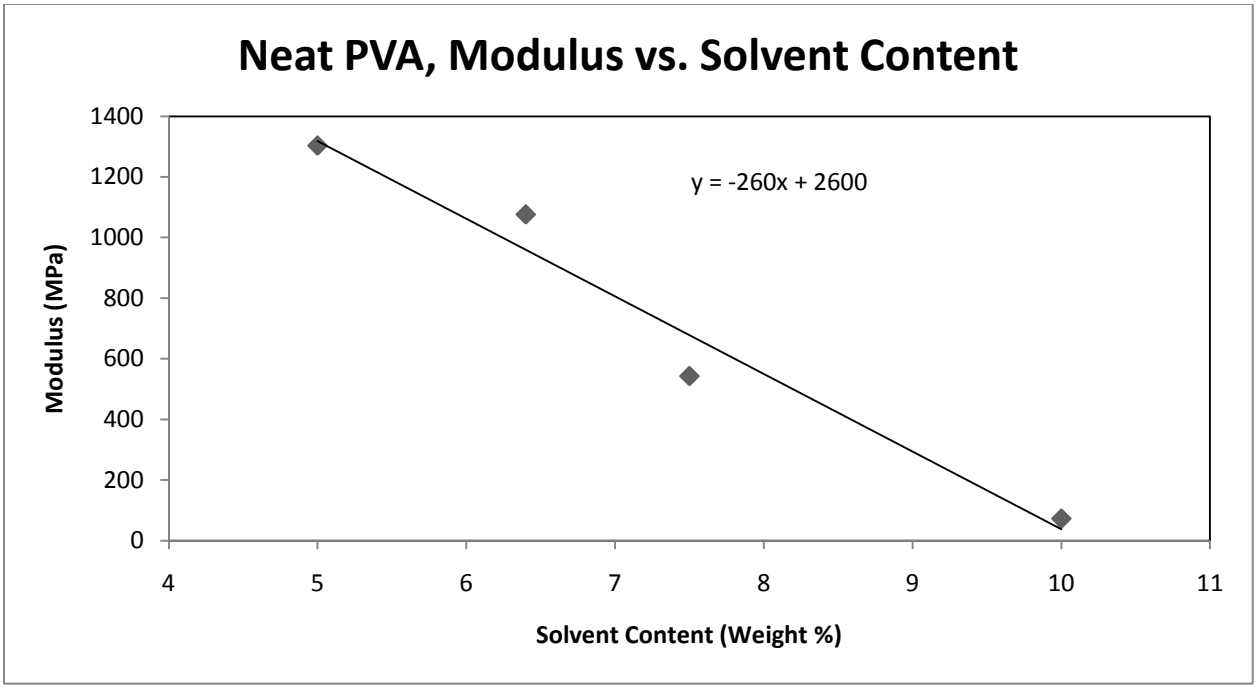

Figure 7: Elongation at Break vs. Solvent Content for Neat PVA

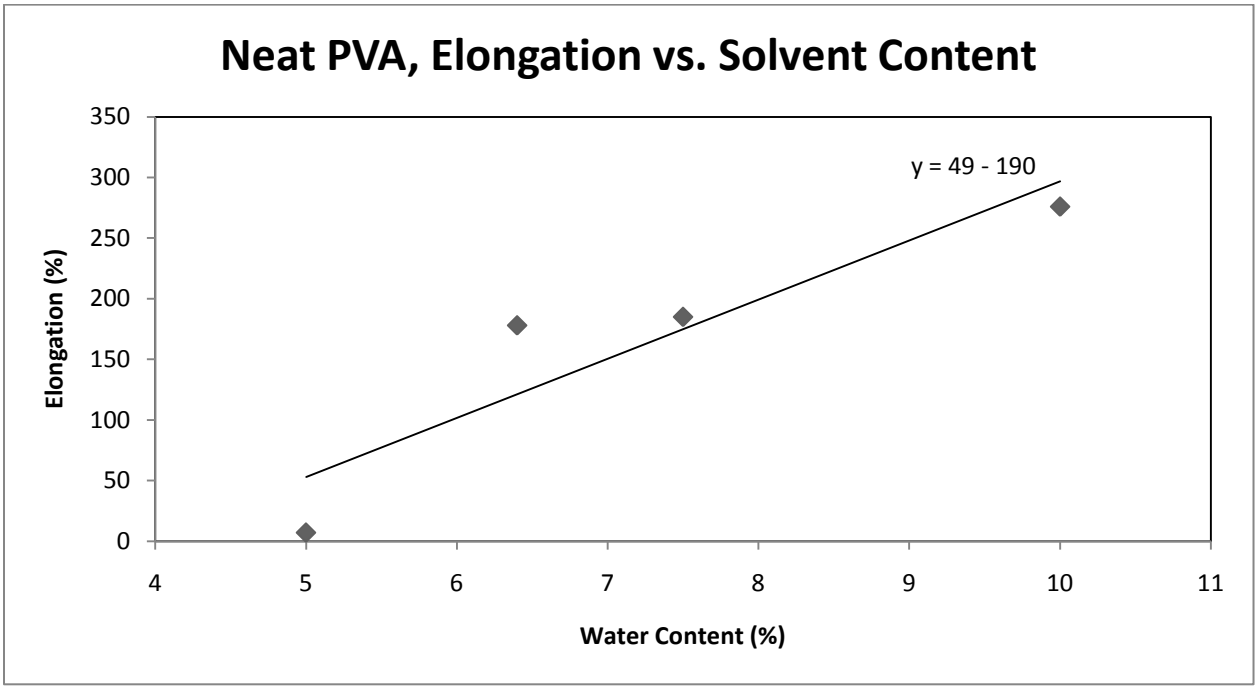

Using these linear best fits from these figures, we can interpolate the modulus and elongation at break values neat PVA at any solvent composition. We wish to compare the mechanical data of the FGS-2 loaded samples to the neat PVA at the same solvent content to remove any possible solvent effects. We use the above linear fits to find the modulus and elongation at break in the neat sample at the solvent amount that correspond to the solvent content of the loaded samples (6.0% and 6.5%). A comparison between these interpolated mechanical values for the neat PVA at these other solvent contents will in theory isolate the effect that FGS-2 has on the mechanical properties. Sample calculations for the interpolation of the neat PVA modulus and percent elongation at 6.5% solvent are shown below.

$$Best\ fit\ equation\ for\ the\ modulus: E = -260\ (Solvent\ content)\frac{MPa}{\%} + 2600 MPa$$

$$E = -260\ (6.5\ \%)\left(\frac{MPa}{\%}\right) + 2600\ MPa = 940\ MPa$$

$$Best\ fit\ equation\ for\ the\ Elong.: Elong. = 49\ (solvent\ content) - 190\%$$

$$\%\ Elongation = 49(6.5\%) - 190\% = 130\ \%$$

The negative intercept in the best fit equation for strain at break seems alarming. It would imply that a sample at low enough solvent concentrations would break before a positive strain is even applied. However, the proportional relationships between the mechanical properties and solvent composition was only found to be true above a certain minimum solvent content.[25] The concentrations which lead to a negative interpolated elongation are more than likely below this minimum solvent content range (and therefore the linear fit does not apply and should not be used).

The interpolation for each concentration is then compared to the loaded samples in Table 4.

Table 3: PVA Comparison of Tensile Properties with Interpolated Equal Solvent Content

PVA Sample	Solvent Content (Weight %)	Modulus (MPa)	Elong. @ Break (%)
1.0 % FGS2	6.5	840	140
Neat (Interpolated)	6.5	940	130
Δ	-	-100	10
0.5% FGS2	6.0	1080	180
Neat (Interpolated)	6.0	1060	100
Δ	-	20	80

Mechanical Testing Results for PMMA

The stress vs. strain plots for the PMMA system are combined and shown below in figures 8, 9, and 10.

Figure 8: Stress Strain Curves for Neat PMMA

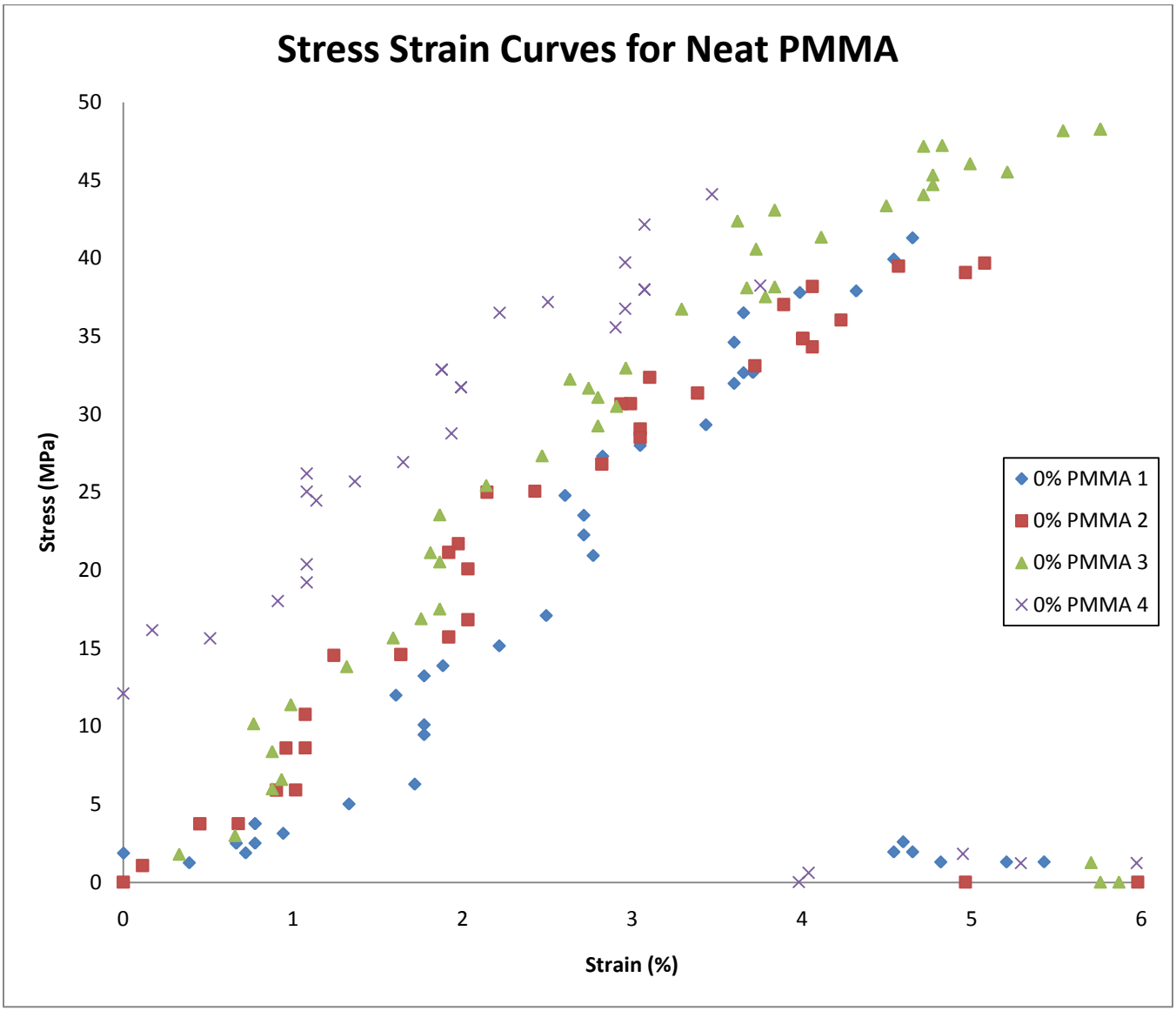

Figure 9: Stress Strain Curves for 0.01% FGS2 in PMMA

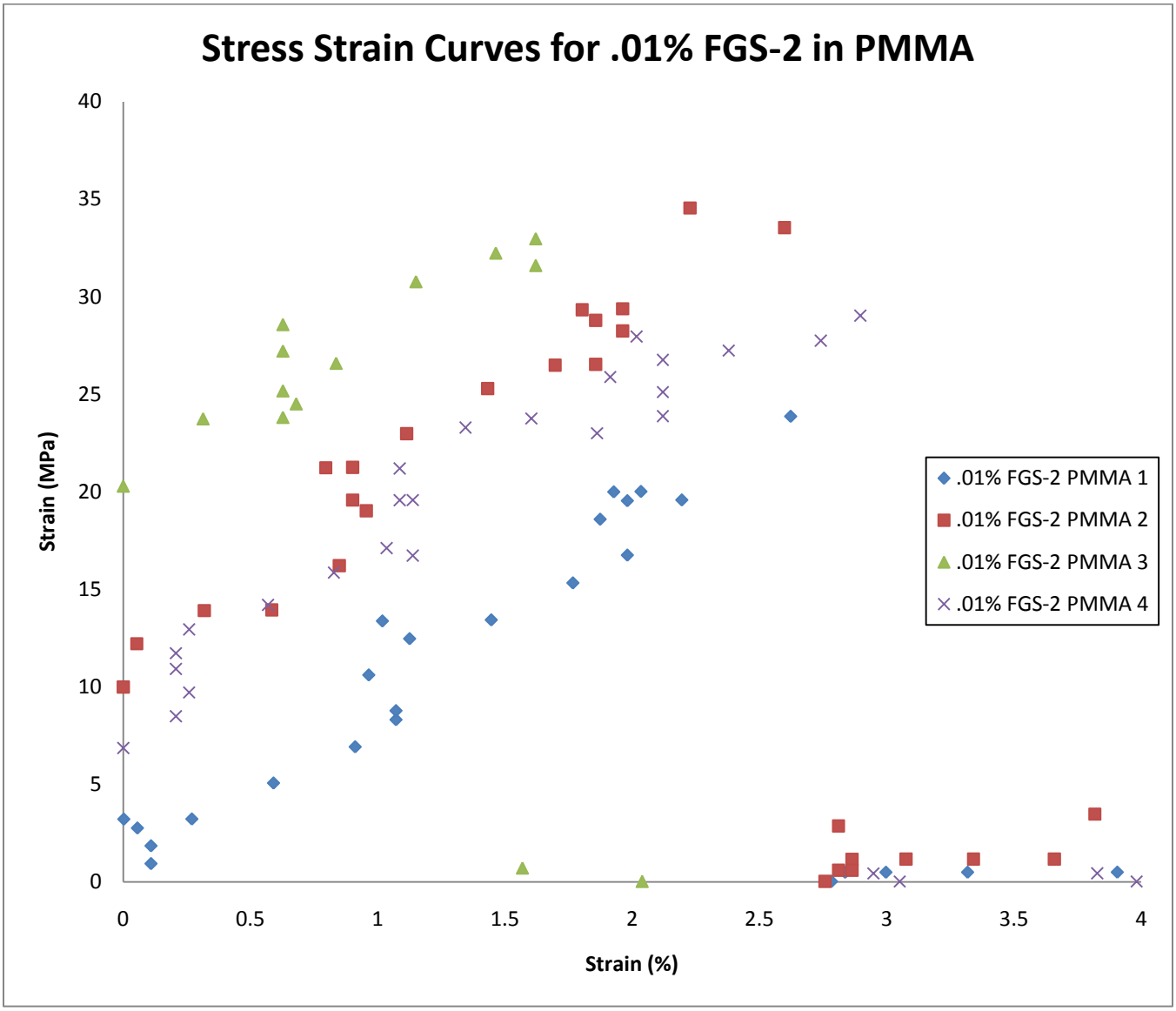

Figure 10: Stress Strain Curves for 0.1% FGS2 in PMMA

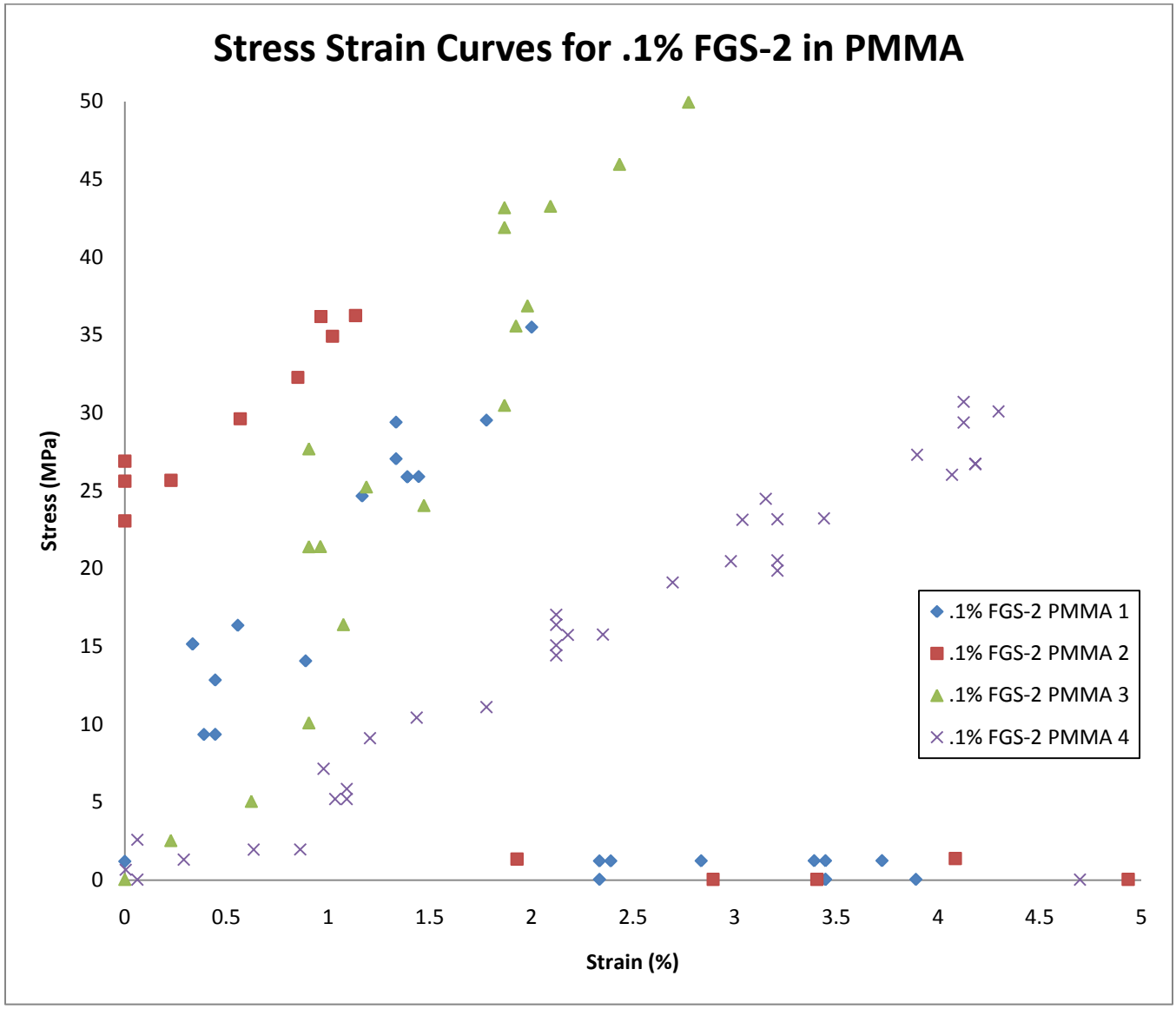

Thermogravimetric analysis was also performed once for each concentration using the same temperature treatment.

A TGA showing the temperature ramp for a neat PMMA sample is depicted in figure 11.

Figure 11: Sample TGA for PMMA

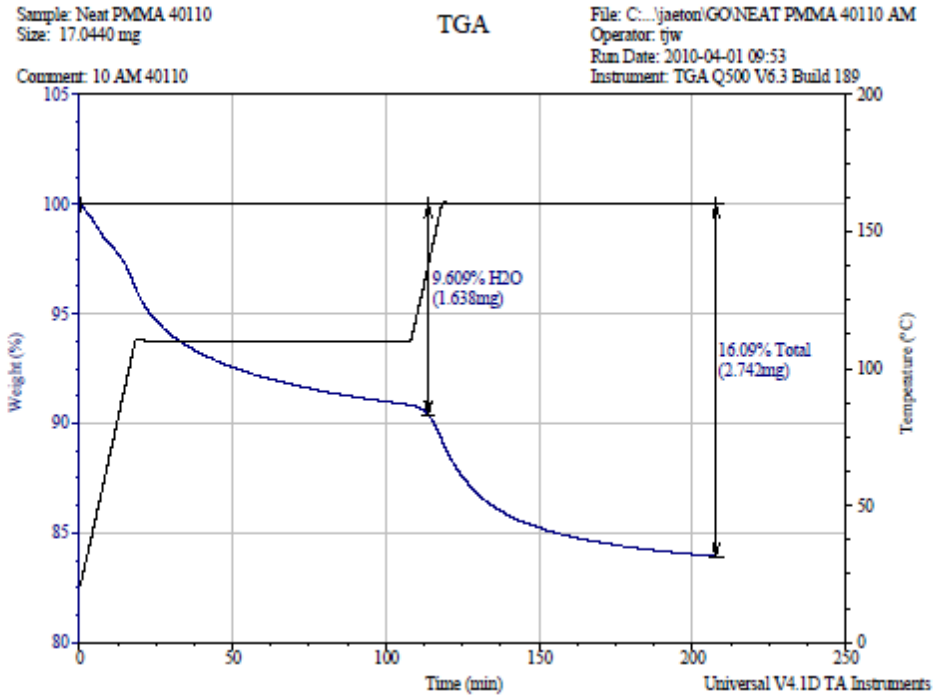

The modulus, strain at break, and stress at break were calculated for each run and averaged for each sample. The relevant results for the PMMA mechanical data are summarized in table 4.

Table 4: Summary of PMMA Results

Sample	Modulus (MPa)	Elong. @ brk. (%)	Stress @ brk. (MPa)	Solvent content (Weight %)
Neat 1	1080	4.2	41	10.7
Neat 2	1050	5.1	40	10.7
Neat 3	1210	5.5	48	10.7
Neat 4	860	3.8	44	10.7
Avg	**1050**	**4.6**	**43**	
St. Dev.	**150**	**0.8**	**4**	
0.01% FGS2 1	870	3.6	24	11.7
0.01% FGS2 2	940	2.6	35	11.7
0.01% FGS2 3	780	1.6	33	11.7
0.01% FGS2 4	820	2.9	29	11.7
Avg	**850**	**2.7**	**30**	
St. Dev.	**70**	**0.8**	**5**	
0.10% FGS2 1	1360	2.0	36	8.9
0.10% FGS2 2	1230	1.1	36	8.9
0.10% FGS2 3	2050	5.1	85	8.9
0.10% FGS2 4	860	4.3	31	8.9
Avg	**1380**	**3.1**	**47**	
St. Dev.	**500**	**1.9**	**26**	

Again, we cannot comment about the effects that FGS-2 has on this polymer system just yet because the solvent contents vary. To correct for this, we also did a study on the effects of the solvent content on the neat PMMA system in the hopes of observing a linear correlation between the modulus and solvent content, like in PVA. In the end, we will just interpolate the mechanical data for the neat PMMA at solvent contents that correspond to the solvent content of the loaded PMMA samples. Again, this will allow a comparison to be made at equal solvent contents and thus show the effect of just the FGS-2 on the mechanical properties of the system.

Table 5: Effect of Solvent Content on Tensile Measurements for PMMA

Solvent Content (Weight %)	Modulus (Mpa)	Elongation @ Break (%)	Stress @ Break (MPa)
10.7	1050	4.6	43
10.8	840	4.0	29
13.1	510	24.7	23
14.0	580	12.2	29
16.1	330	49.7	20

Figure 12: Modulus vs. Solvent Content for Neat PMMA

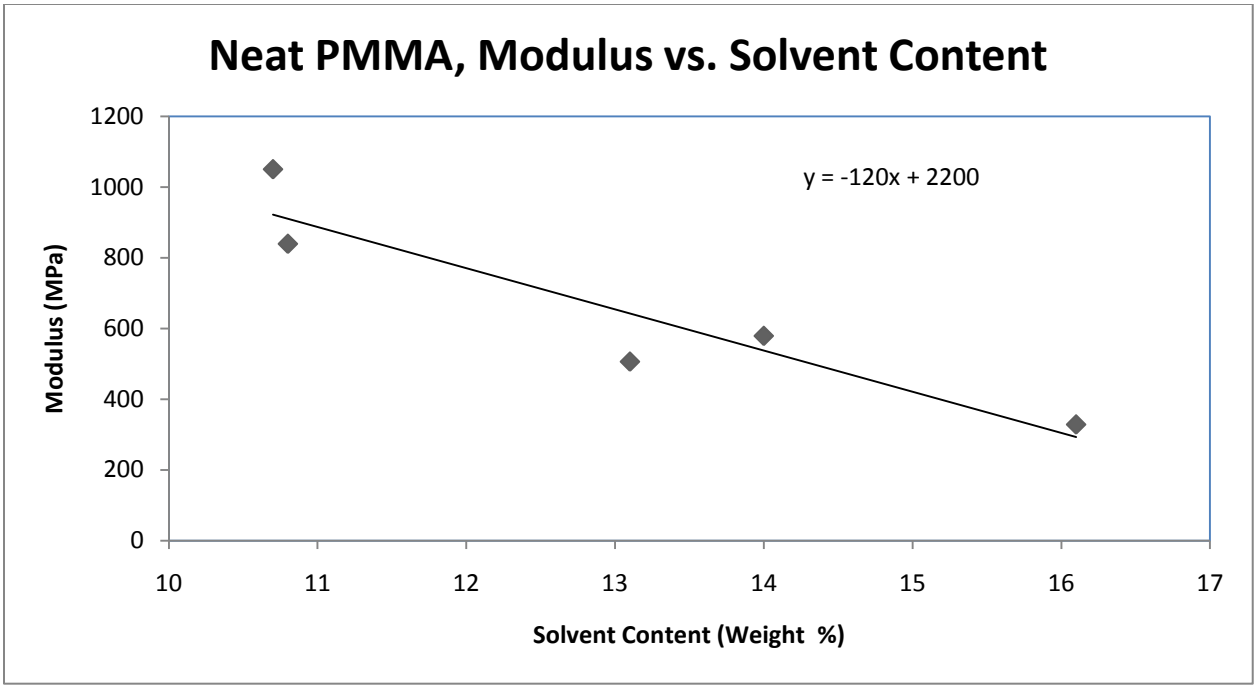

Figure 13: Elongation at Break vs. Solvent Content for Neat PMMA

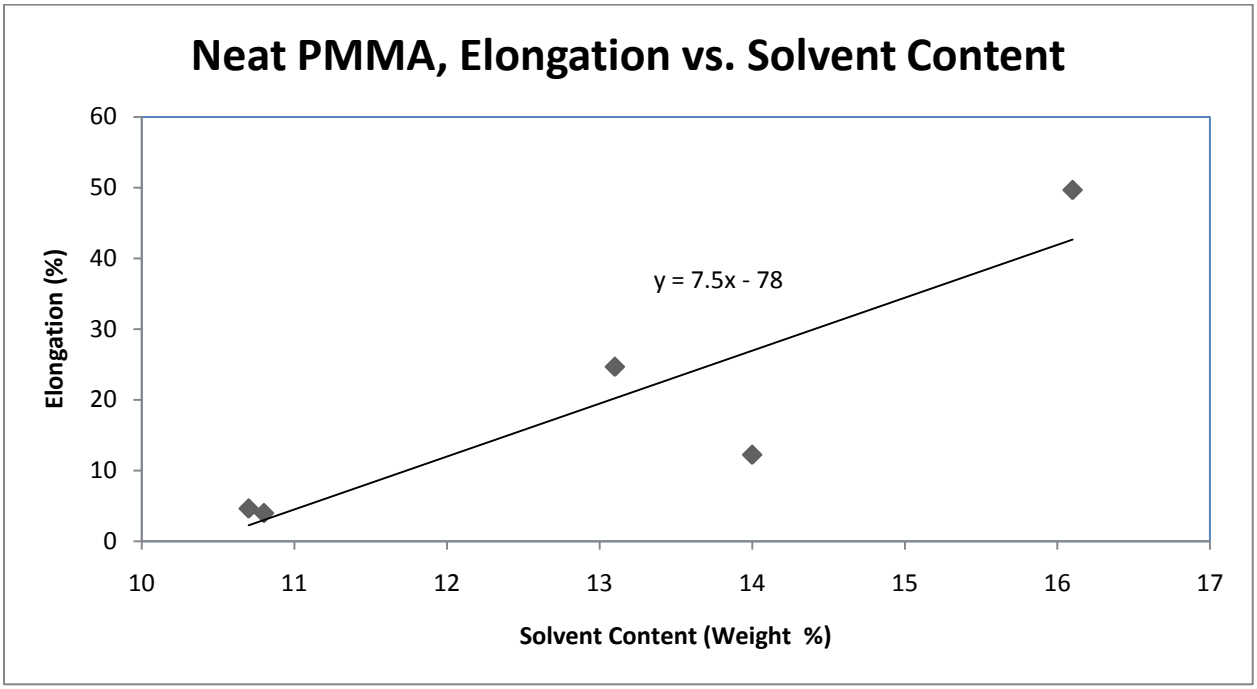

Figure 14: Stress at Break vs. Solvent Content for Neat PMMA

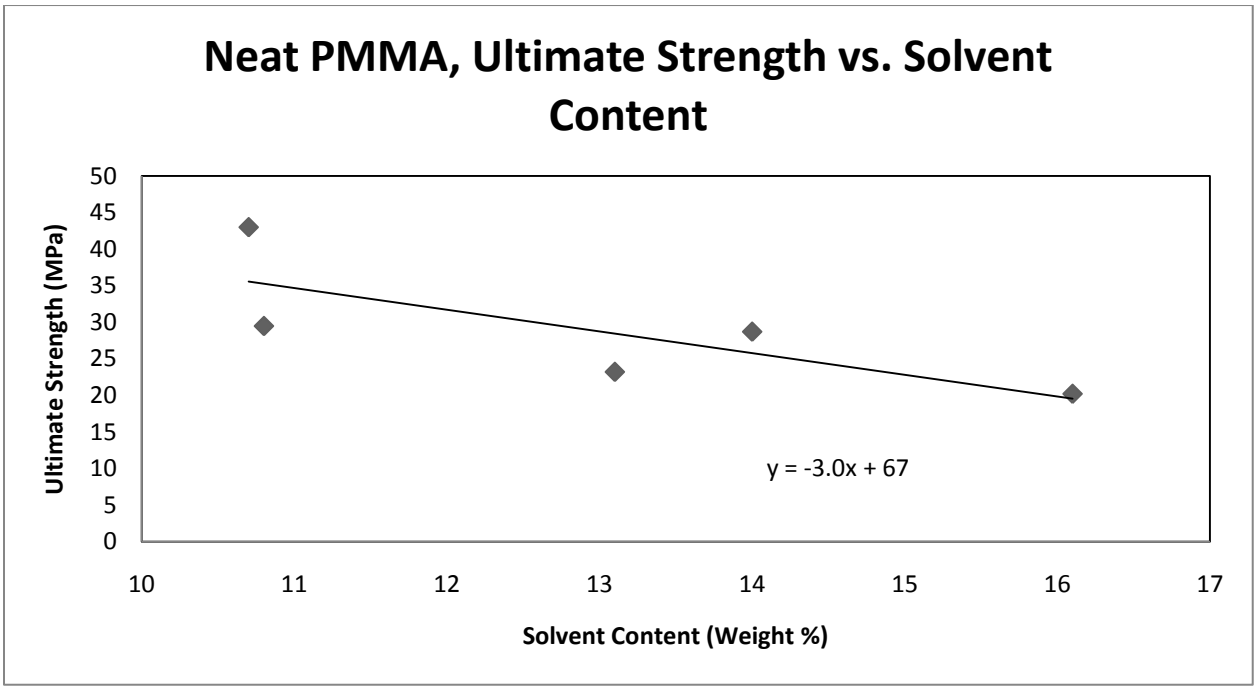

Again we construct a table interpolating the modulus and elongation values for the neat polymer at the solvent contents of the other compositions to eliminate the effects that result from the different solvent contents between samples.

Table 6: PMMA Comparison of Tensile Properties with Interpolated Equal Solvent Content

PMMA Sample	Solvent Content (Weight %)	Modulus (MPa)	Elong. @ Break (%)	Stress @ Break (MPa)
0.1 % FGS2	8.9	1380	3.1	47
Neat (Interpolated)	8.9	1130	-11.2	41
Δ	-	250	13.9	6
0.01% FGS2	11.7	850	2.7	30
Neat (Interpolated)	11.7	810	9.7	33
Δ	-	40	-7.0	-3

Interestingly, the interpolated elongation at break for our concentrations is negative. This implies that a neat sample at 8.9% solvent content at that length would have broken before a stress is even applied, or the initial sample length would have shrunk by at least 11.2%.

Mechanical Testing Results for PEI

The initial preparation of PEI was noticeably unsuccessful. The polymer is supposed to be amorphous (clear), but the presence of large amounts of water in the film made our first batch of samples cloudy and opaque. For glass transition temperature measurements, new films were created that were transparent as expected by amending the preparation method. However, mechanical tests were still performed on the original films, and the following data is of that first batch. The stress vs. strain plots for the PEI system are combined and shown below in figures 15, 16, and 17.

Figure 15: Stress Strain Curves for Neat PEI

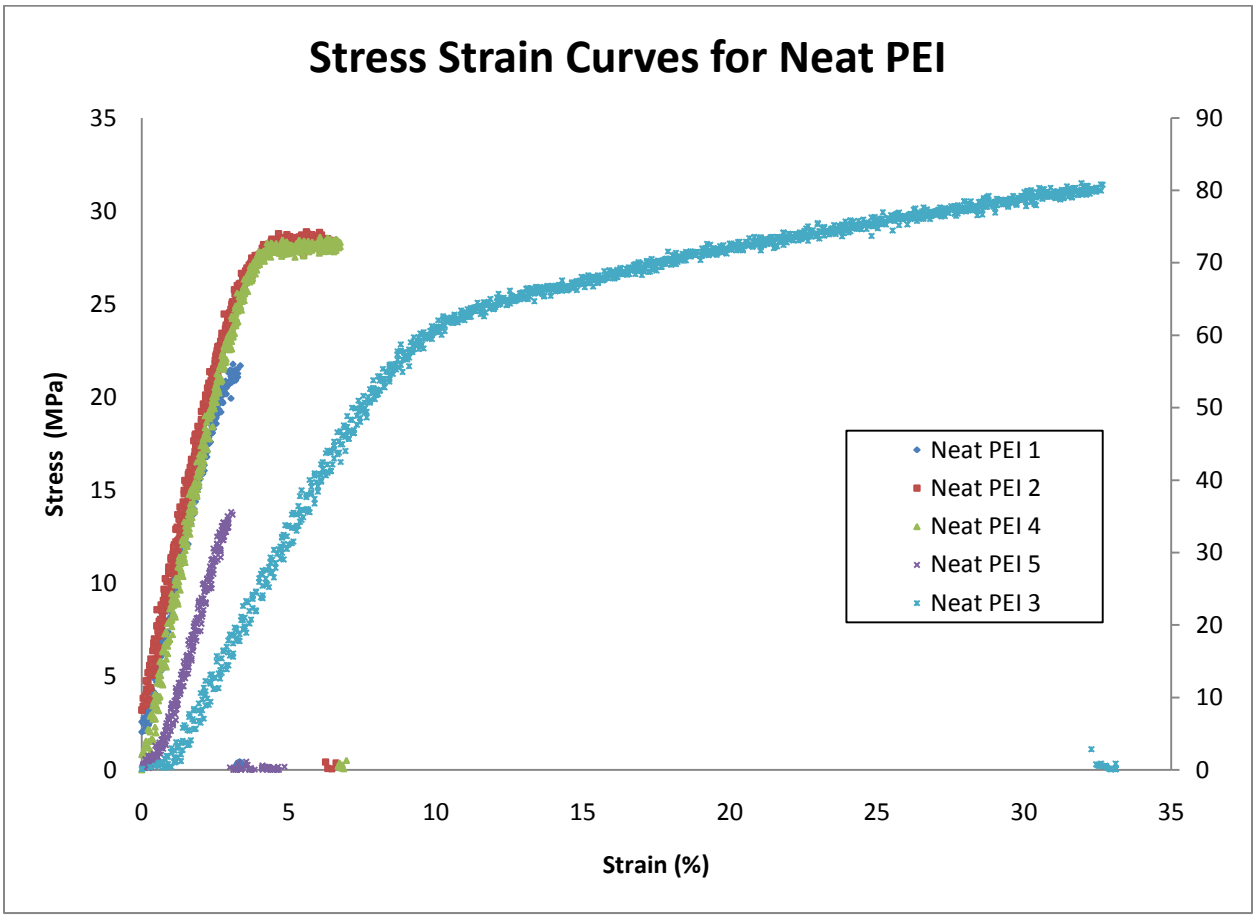

Note: The values for Neat PEI 3(shown by the light blue "x") sample were uncharacteristically high. To ensure visual resolution of the plot, the stress of this series is plotted on the right axis. This sample is

still included in calculations because despite its high stress and strain at break, its modulus still is within the range of the other four measurements.

Figure 16: Stress Strain Curves for 0.05% FGS2 in PEI

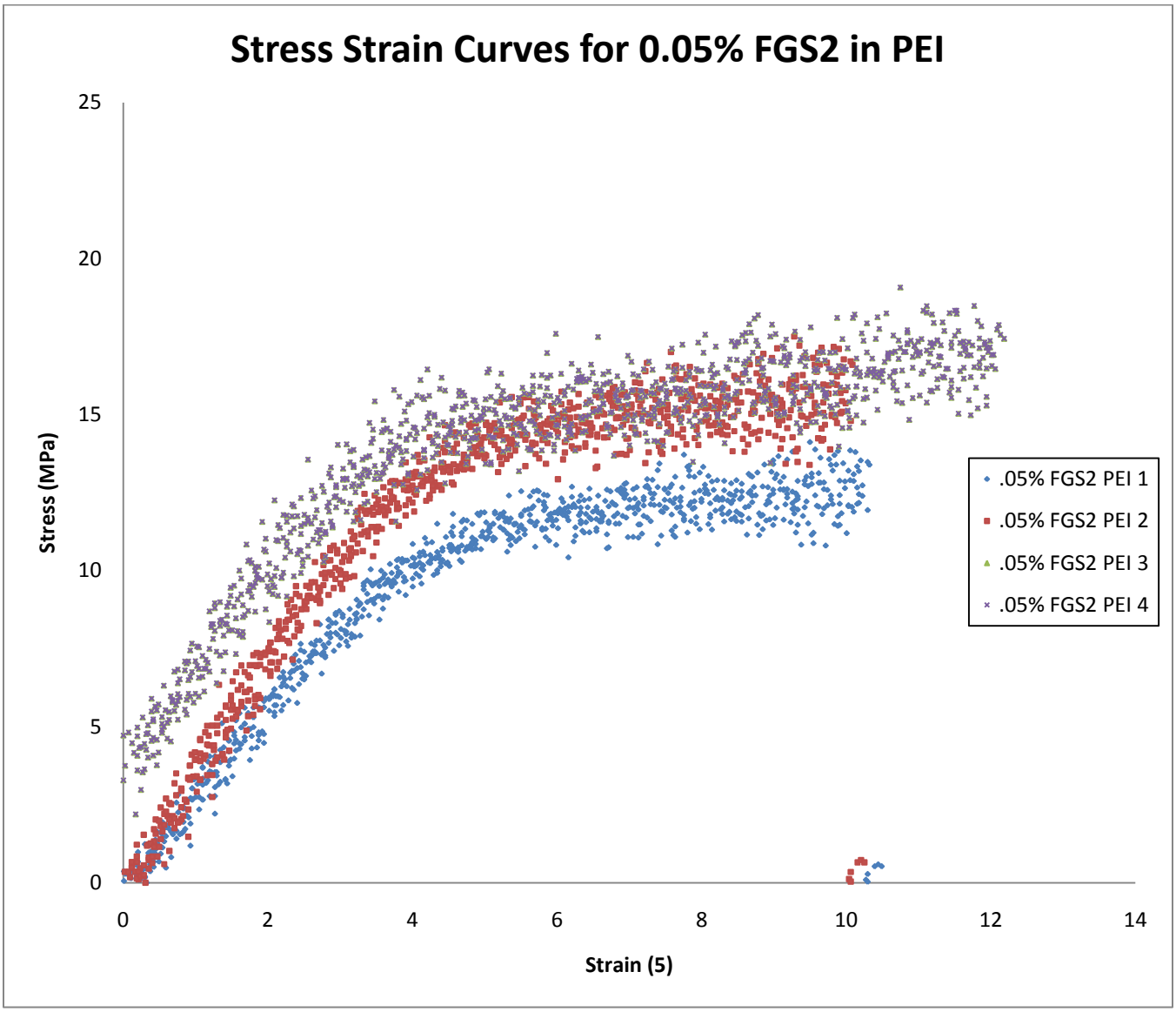

Figure 17: Stress Strain Curves for 0.1% FGS2 in PEI

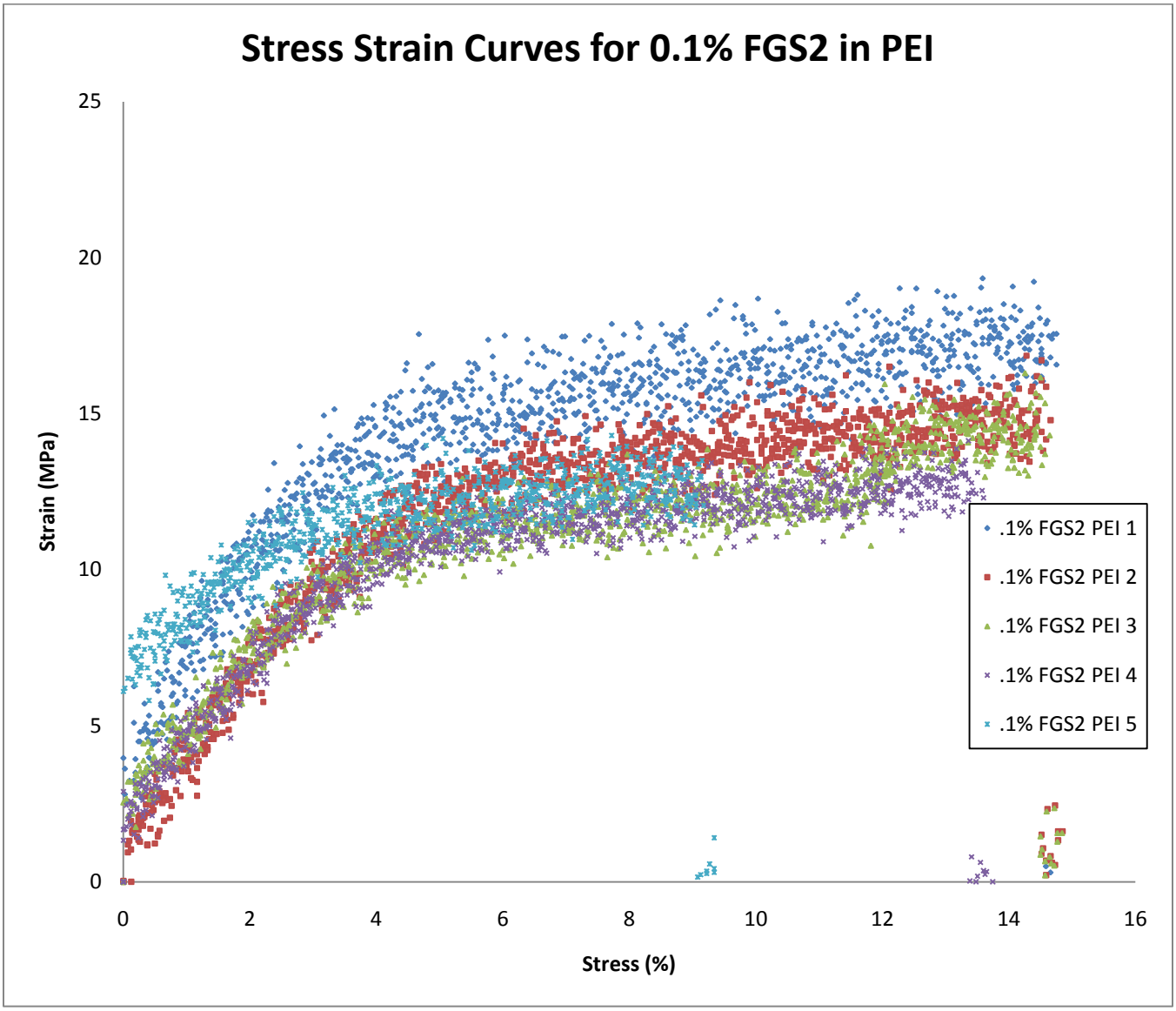

Table 7: Summary of PEI Results

Sample	Modulus (MPa)	Elong. @ brk. (%)	Stress @ brk. (MPa)	Solvent content (Weight %)
Neat 1	730	3	22	11.4
Neat 2	760	6	28	11.4
Neat 3	740	31	80	11.4
Neat 4	830	7	28	11.4
Neat 5	500	3	14	11.4
Avg	**710**	**10**	**34**	
St. Dev.	**120**	**12**	**26**	
0.05% FGS2 1	280	15	16	5.9
0.05% FGS2 2	390	11	17	5.9
0.05% FGS2 3	340	12	19	5.9
0.05% FGS2 4	260	15	18	5.9
Avg	**320**	**13**	**18**	
St. Dev.	**60**	**2**	**1**	
0.10% FGS2 1	250	12	14	6.8
0.10% FGS2 2	270	15	17	6.8
0.10% FGS2 3	220	15	16	6.8
0.10% FGS2 4	260	13	14	6.8
0.10% FGS2 5	190	9	14	6.8
Avg	**240**	**13**	**15**	
St. Dev.	**30**	**2**	**2**	

Figure 18 depicts a TGA of a PEI sample. This same temperature ramp method was used in all PEI solvent measurements.

Figure 18: Sample TGA for PEI

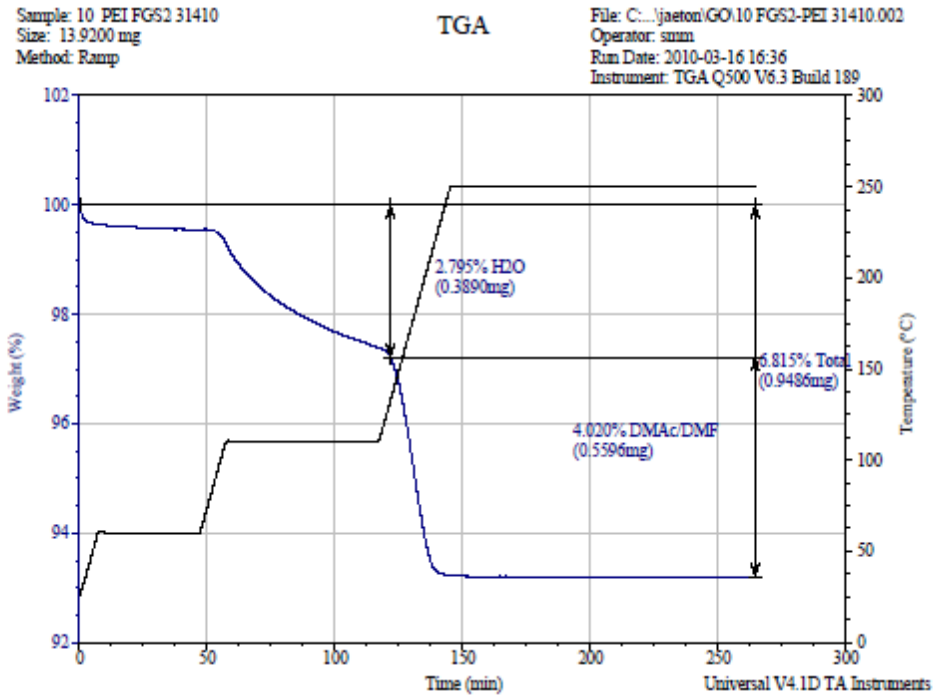

A study of possible solvent content is not necessary for the PEI system. The modulus of a polymer almost always decreases as the solvent content increases. However, even with a lower solvent content, FGS2 loaded PEI has a lower modulus than neat PEI. Thus, it is already obvious that FGS2 will not enhance all of the tensile properties of PEI.

Glass Transition Temperature Results

In order to comment on the thermal resistance of the nanocomposite systems, glass transition temperature measurements were made using a differential scanning calorimeter. The following figures are the resulting plots.

Figure 19: Neat PVA Glass Transition Temperature Measurement by DSC

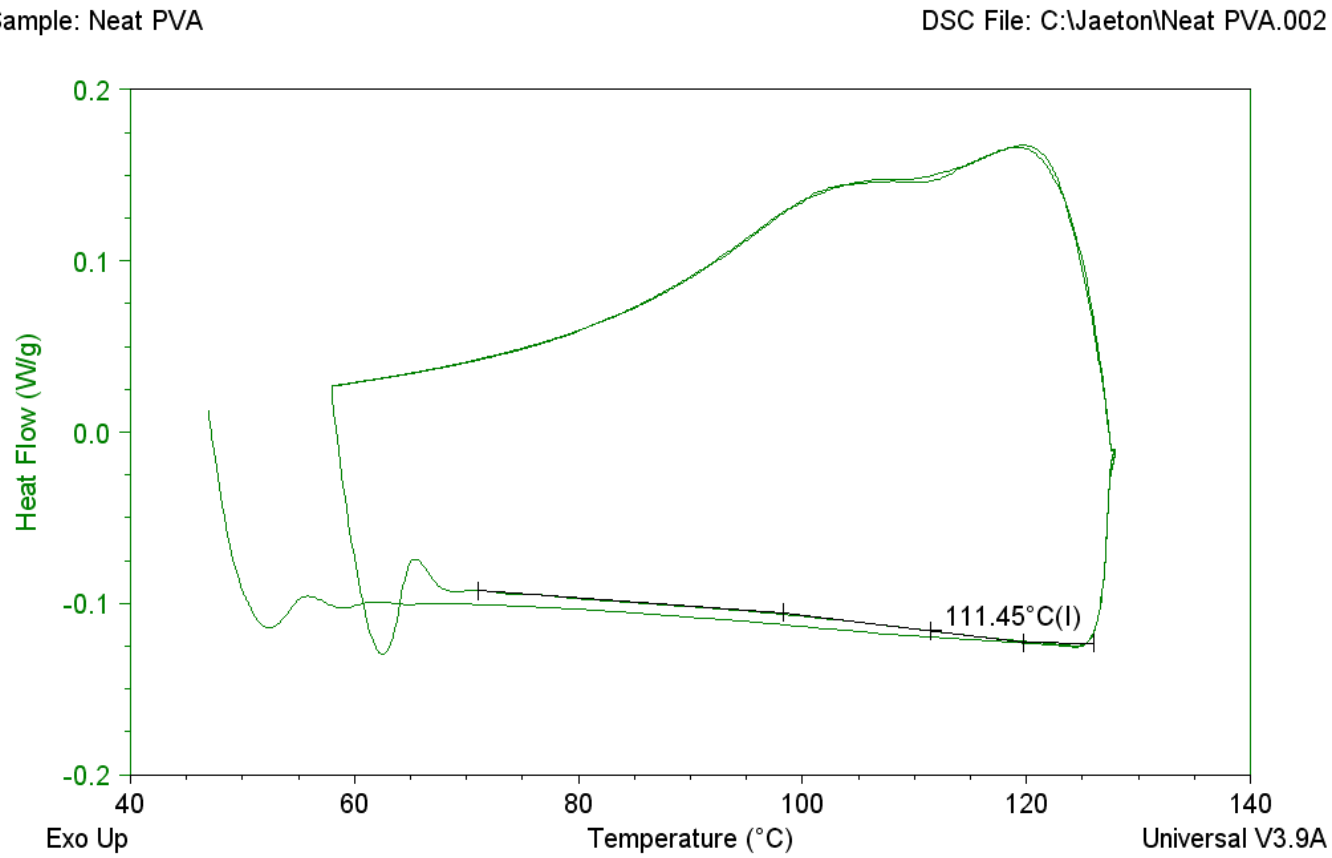

Figure 20: 1.0% FGS2 in PVA Glass Transition Temperature Measurements by DSC

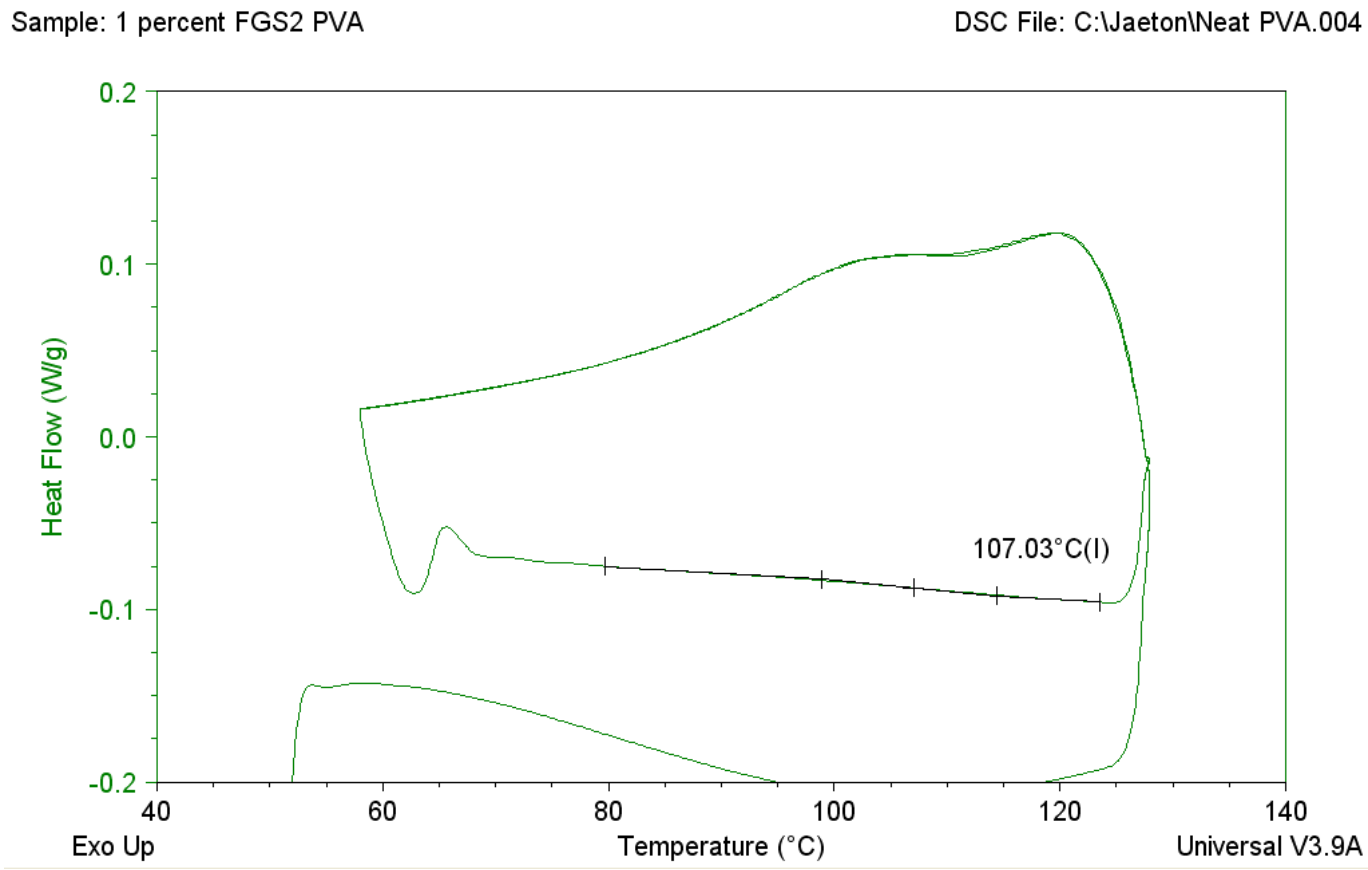

Figure 21: Neat PMMA Glass Transition Temperature Measurement by DSC

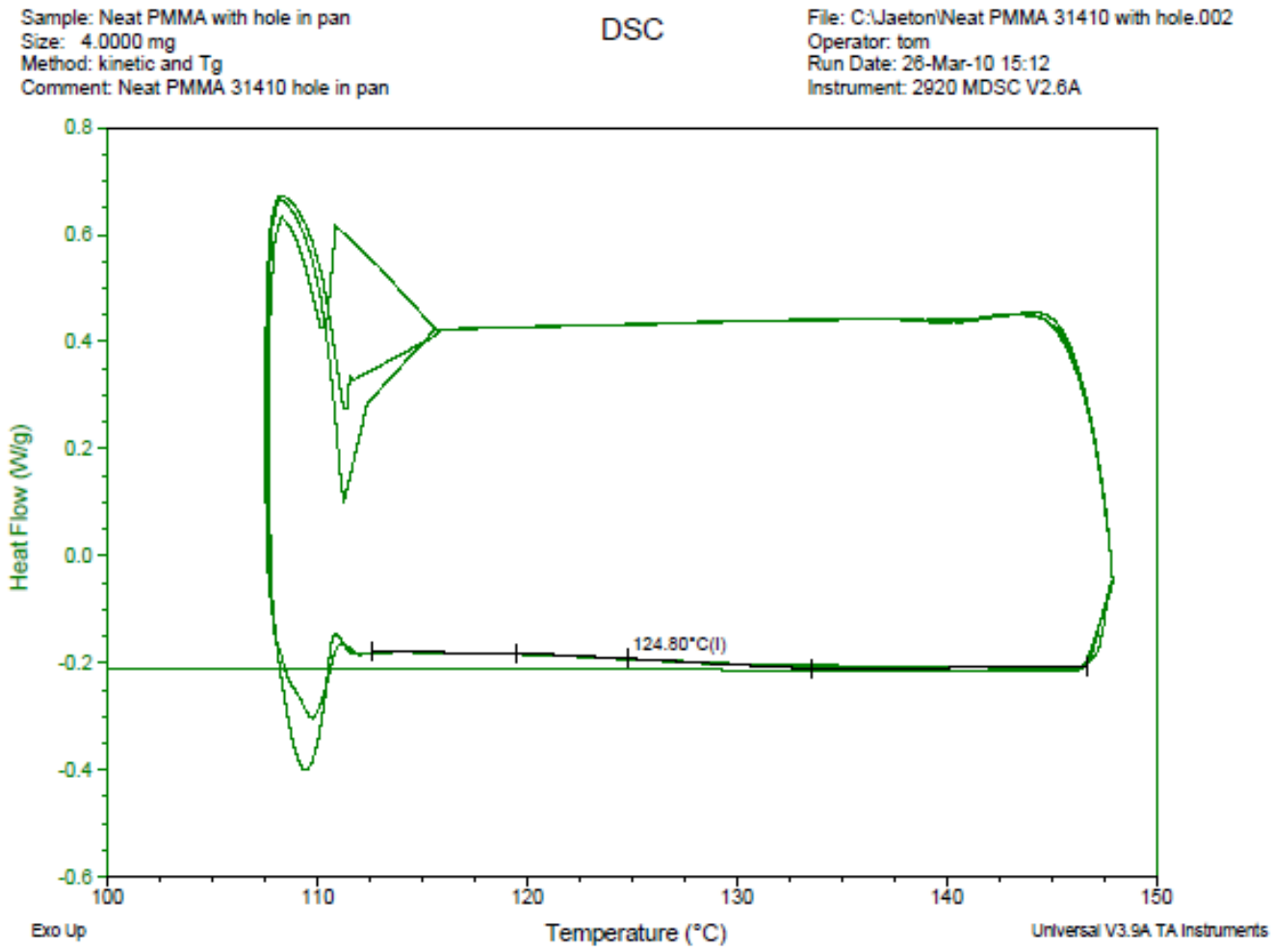

Figure 22: 0.2% FGS2 in PMMA Glass Transition Temperature Measurement by DSC

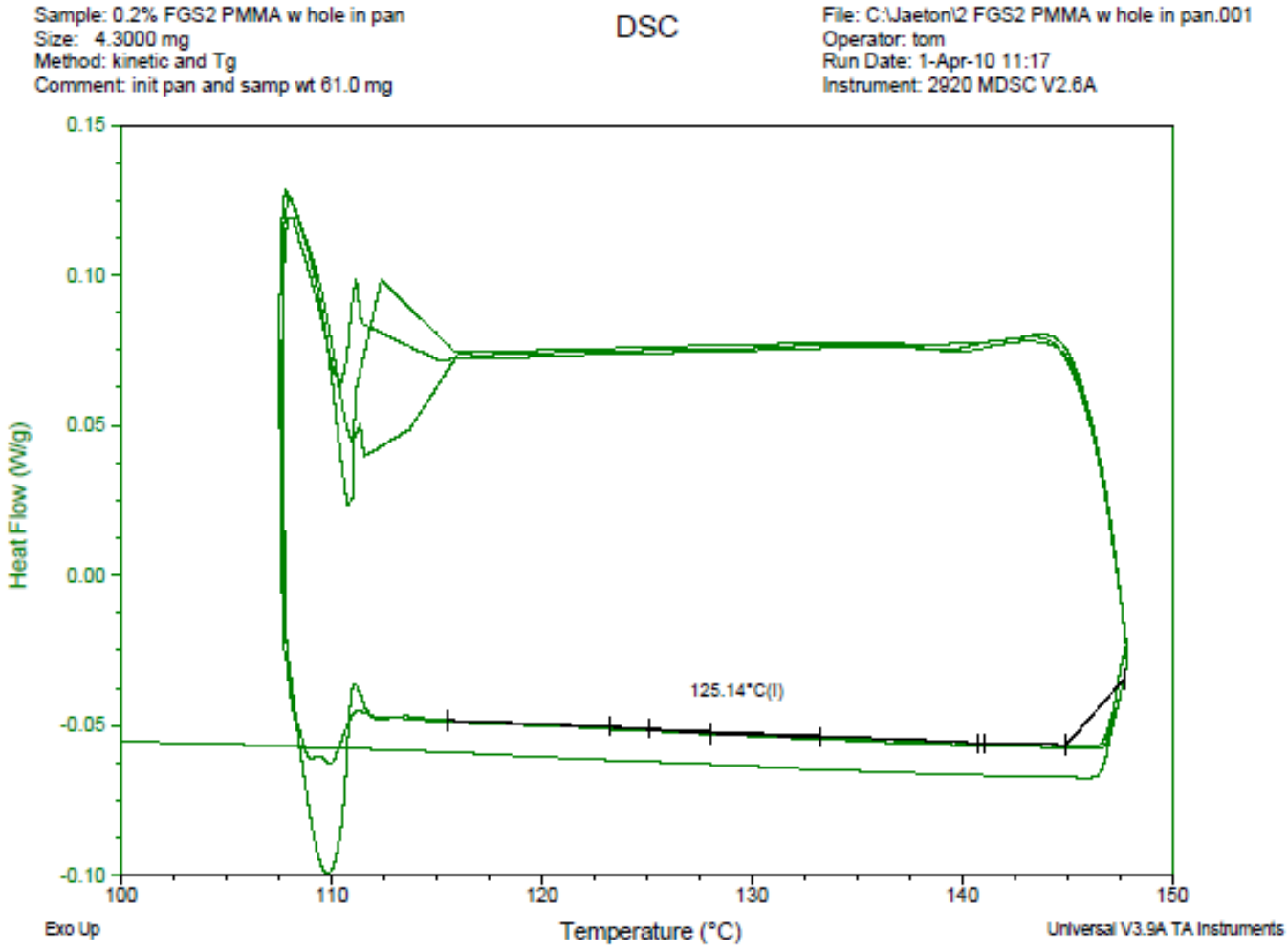

Figure 23: Neat PEI Glass Transition Temperature Measurement by DSC

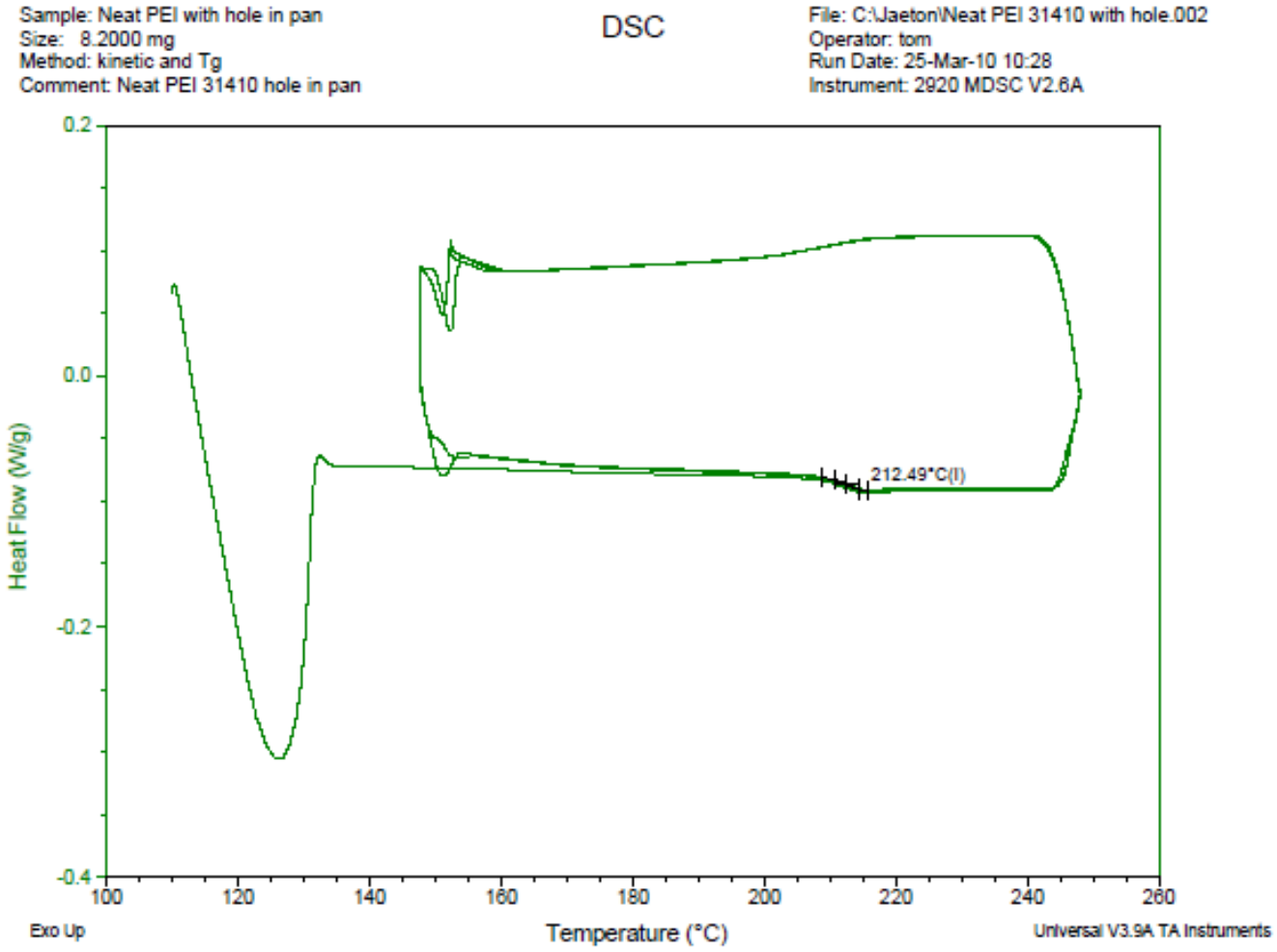

Figure 24: 0.1% FGS2 in PEI Glass Transition Temperature Measurement by DSC

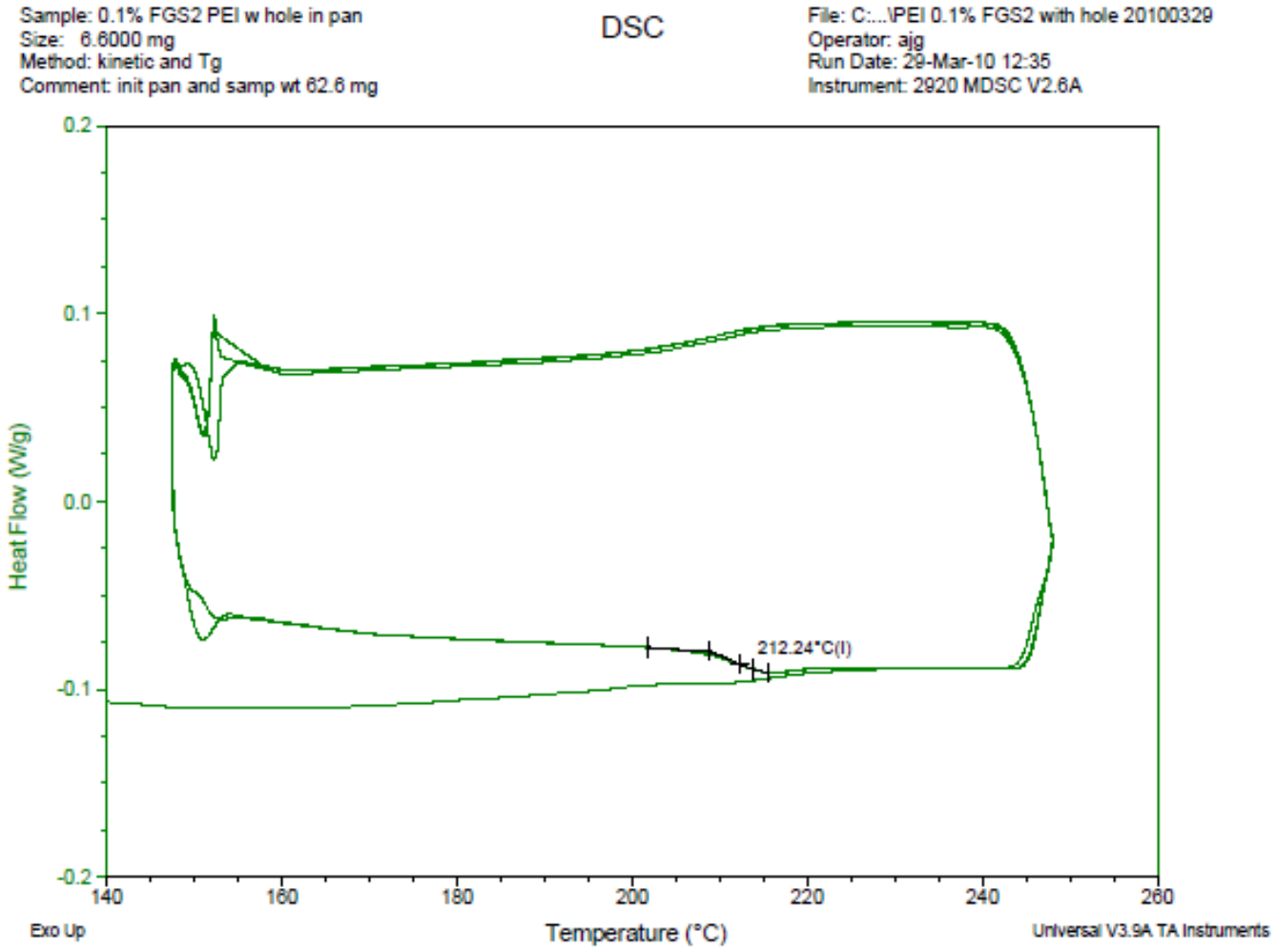

Table 8: Summary of Glass Transition Temperature Results

Sample	T_g (˚C)	Sample	T_g (˚C)	Sample	T_g (˚C)
Neat PVA	111.5	Neat PMMA	124.8	Neat PEI	212.5
1.0% FGS2 in PVA	107.0	0.2% FGS2 in PMMA	125.1	0.1% FGS2 in PEI	212.2
Δ	-4.5	Δ	0.3	Δ	-0.3

Discussion

The initial results of this study are incredibly successful. We managed to develop a method for adding functionalized graphene sheets to all three polymers while maintaining the desired dispersion. We also saw that for PVA and PMMA, certain concentrations of FGS-2 improved the performance of the composite. Also, the interfacial interaction measurements may help predict the effect of FGS-2 in certain polymers as the weakest interaction strength occurred in PEI, the same polymer which saw the largest decrease in performance in the loaded composite films.

The PVA preparation first proved that we can add FGS into the PVA system without using an organic solvent. The mechanical tests with the interpolated data to remove solvent contribution, demonstrated that the addition of only 0.05% FGS2 to the neat PVA system results in a slight increase in modulus (of about 20MPa) and a substantial increase in elongation at break (around an additional 80% elongation). However, the 0.10% FGS2 in PVA polymers saw a substantial drop in the modulus of 100 MPa, and a slight increase of 10% in the average elongation from the neat PVA. Thus, there exists an optimal concentration of FGS in PVA that would improve the mechanical performance!

PMMA demonstrated, as desired, an improvement in mechanical properties with the addition of FGS2 when compared to the interpolated values neat system. With only 0.01% FGS2 composition by weight, the modulus increased by 40 MPa. However this increase in stiffness led to a decrease in elongation at break (from 9.7% to only 2.7%) and 3 MPa decrease in the stress at break. For the more loaded PMMA film of 1.0% FGS2, we saw a dramatic increase of 250 MPa in the modulus, a 6 MPa increase in ultimate strength, and a theoretical improved elongation! However, the interpolation for the elongation at break for the neat system does not inspire much confidence and the linear interpolation might not hold for this system. The least solvent dependent measurement, the glass transition temperature, also showed an improvement from the neat system as the glass transition temperature rose slightly (less than a degree) for the nanocomposite. This result suggests that the

presence of FGS increases the resistance of PMMA to high temperatures. This observed increase in T_g is far less than the 30˚C at all FGS loadings above 0.05% observed previously [1]. Several factors cause this discrepancy. One source of error is the inherent dependence of T_g on the method, particularly the rate of heating and cooling[25]. It is very possible that our rate of 3˚C was different from the rate used for the previous measurements. Also, the FGS we used had a much lower C:O ratio and is therefore more polar. This change in surface chemistry would easily cause the interactions and measured glass transition temperature to differ. Regardless, we did achieve our initial goal by finding a weight concentration of FGS2 in PMMA that can improve all the measured mechanical properties and the thermal resistance!

Our results show that PEI performed worse with the addition of FGS2. The modulus plummeted almost 400 MPa at the smallest concentration of FGS2. The modulus continued to drop as we increased the concentration to 0.1% FGS2, even though the solvent composition decreased (a trend that encourages an increase in the modulus for the other polymer systems!). The stress at break similarly decreases sharply with the addition of FGS2. The glass transition temperature of the PEI nanocomposite was also lower than the neat polymer. Thereby weakening the thermal resistance of PEI, a polymer often used for its thermal stability!

In order to rationalize the mechanical results, we can look to the interfacial interaction strength measurements. The nanoparticle-polymer interfacial interaction was qualititatively measured to be weakest with PEI. Although the film quality has not reached an ideal level, we see this weak interfacial interaction strength between FGS-2 and PEI coincides with poor mechanical performance in the loaded samples. The presence of noninteracting sheets in system may be thought of as tiny holes in the polymer system, causing it to fail easier. However, we do notice that even though PVA was observed to have a stronger particle interaction than PMMA, at 0.1% FGS by weight compositions, PMMA shows a

larger improvement in more properties. The presence of a more complicated interaction (such as so called "slip planes"[2]) than just the measured interfacial interaction could explain this result.

It should be noted that the above interpretations of the results assume that the solvent-FGS2 did not interact in a way that affects the mechanical properties. We failed to create a method that drove off all the solvent. In the case of PMMA films, extended exposure (of over a week) to the dry box did not reduce the solvent content any further than the measured values. For the preparation of PEI composites, we similarly found that the solvent content leveled off even with extended heat treatment. We cannot simply increase the temperature of the heat treatment as we are concerned with degrading the polymer or reducing the FGS. The use of a vacuum oven could help ameliorate the sample preparation by allowing us to drive off more solvent at lower temperatures.

The glass transition temperature measurements also generally agree with the interfacial interaction measurements as the stronger particle-polymer interaction in PMMA shows an increase in thermal resistance while the weakly interacting PEI does not. However, we note that PVA, the polymer with the strongest interaction shows a large drop in T_g. This drop can be attributed to the unusually high concentration of FGS2 in the measured PVA sample. One would expect that as you increase the nanoparticle composition, the sheets would actually interfere with the interchain interactions of the polymer to such an extent that the glass transition temperature would drop. A study of a smaller concentration (for example 0.1% FGS2 in PVA) may show drastically different results.

The FGS2 concentration on a whole shows to have marked effects on the mechanical properties as well. We can clearly see that even in the polymers that showed some improvements, the overall performance varies greatly with composition. The performance improvement occurs at the lower concentrations of FGS2 (0.05% rather than 0.1%) for PVA, while the higher concentrated (0.1%) outperforms the lower concentrated (0.01%) FGS2 PMMA sample. Thus, there seems to be a

mechanically optimal weight composition of FGS2 for these polymers that the study of additional concentrations can ascertain.

Acknowledgements

I am thankful to Minzhen Cai for her help preparing, exfoliating and dispersing the FGS starting with graphite. Her work with atomic force microscopy characterized the polymer-particle interactions, allowing for a better understanding of the systems under study.

Thanks to Arthur Jaeton Glover for his work on the PVA system and constant help and advice along every step of this research.

And of course, I am grateful for the support of Professor Hannes Schniepp and Professor David Kranbuehl, whose experience, patience, knowledge and continued encouragement was invaluable to me throughout this process.

References

1. Ajayan, P.M.; Schadler, L.S.; Braun, P.V.; Nanocomposite Science and Technology. Wiley Publishing Co.: **2007**. 1.
2. Ramanathan, T.; Abdala, A.; Stankovich, D.; Dikin, A.; Herrera-Alonso M.; Piner, R.; Adamson, H.; Schniepp, H.; Chen, X.; Ruoff, R.; Nguyen, S.; Aksay, I.; Prud'Homme, R.; Brinson, L. Functionalized graphene sheets for polymer nanocomposies. *Nat Nano Lett.* **2008***, 3*. 327 -331
3. Stankovich, S.; Dikin, D.; Dommet, G.; Kohlhass, K.. Zimney, E.; Stach, E.; Piner, R.; Nguyen, S.; Ruoff, R. Graphene-based composite material. *Nature*. **2006**, *442*, 282-288
4. Ajayan, P. M.; Tour, J. M., Nanotube Composites. *Nature* **2007**, *447*, 1066–1068
5. Ajayan, P. M.; Schadler, L., S.; Giannaris, C.; Rubio, A., Single-Walled Carbon Nanotube– Polymer Composites: Strength and Weakness. *Adv. Mater*. **2000**, *12*, 750–753.
6. Lan, T.; Pinnavaia, T. J., Clay-Reinforced Epoxy Nanocomposites. *Chem. Mater*. **1994**, *6,* 2216–2219.
7. Ramanathan, T.; Abdala, A. A.; Stankovich, S.; Dikin, D. A.; Herrera-Alonso, M.; Piner, R. D.; Adamson, D. H.; Schniepp, H. C.; Ruoff, R. S.; Nguyen, S. T.; Aksay, I. A.; Prud'homme, R. K.; Brinson, L. C., Functionalized Graphene Sheets for Polymer Nanocomposites. *Nat*. *Nanotechnol*. **2008**, *3*, 327–331.
8. Official Energy Statistics from the U.S. Government, Energy Information Administration, *Annual Energy Review (AER*) **2007**, Report No. DOE/EIA-0384(2007), posted: June 23, 2008.
9. Narula, C. K.; Allison, J. E.; Bauer, D. R.; Gandhi, H. S., Materials Chemistry Issues Related to Advanced Materials Applications in the Automotive Industry. *Chem. Mater*. **1996**, *8,* 984–1003.

10. Miller, W. S.; Zhuang, L.; Bottema, J.; Wittebrood, A. J.; Smet, P. D.; Haszler, A.; Vieregge, A., Recent development in aluminium alloys for the automotive industry. *Mater. Sci. Eng., A: Struct. Mater*. **2000**, *280*, 37–49.

11. Toensmeier, P. A., Advanced composites soar to new heights in Boeing 787. *Plastics Eng*. **2005**, *61*, 8–14.

12. McAllister, M.; et al. Single Sheet Functionalized Graphene by Oxidation and Thermal Expansion of Graphite.*Chem. Mater.* **2007**, *19*, 4396-4404.

13. Weisenberger M. C.; Grulke, E. A.; Jacques, D.; Rantell, T.; Andrews, R. Enhanced Mechanical Properties in Polyacrylonitrile/Multiwall Carbon Nanotube Composite Fibers. *J Nanosci. Nanotechnol.* **2003,** *2,* 535

14. Li, V. C., From Micromechanics to Structural Engineering—The Design of Cementitious Composites for Civil Engineering Applications. *Structrual Eng./Earthquake Eng*. **1993**, *10*, 37s–48s.

15. Kanda, T.; Li, V. C., Practical Design Criteria for Saturated Pseudo Strain Hardening Behavior in ECC. *Journal of Advanced Concrete Technology* **2006**, *4*, 59–72.

16. Schniepp, H. C.; Li, J.-L.; McAllister, M. J.; Sai, H.; Herrera-Alonso, M.; Adamson, D. H.; Prud'homme, R. K.; Car, R.; Saville, D. A.; Aksay, I. A., Functionalized Single Graphene Sheets Derived from Splitting Graphite Oxide. *J. Phys. Chem*. *B* **2006**, *110*, 8535–8539.

17. McAllister, M.; Li, J.-L.; Adamson, D. H.; Schniepp, H. C.; Abdala, A. A.; Liu, J.; Herrera- Alonso, M.; Milius, D. L.; Car, R.; Prud'homme, R. K.; Aksay, I. A., Single Sheet Functionalized Graphene by Oxidation and Thermal Expansion of Graphite. *Chem. Mater*. **2007**, *19*, 4396–4404.

18. Kudin, K. N.; Ozbaz, B.; Schniepp, H. C.; Prud'homme, R. K.; Aksay, I. A.; Car, R., Raman spectra of graphite oxide and functionalized graphene sheets. *Nano Lett*. **2008**, *8*, 36–41.

19. Stankovich, S.; Dikin, D. A.; Dommett, G. H. B.; Kohlhaas, K. M.; Zimney, E. J.; Stach, E. A.; Piner, R. D.; Nguyen, S. T.; Ruoff, R. S., Graphene-based composite materials. *Nature* **2006**, *442*, 282–286.

20. Stankovich, S.; Piner, R. D.; Chen, X.; Wu, N.; Nguyen, S. T.; Ruoff, R. S., Stable aqueous dispersions of graphitic nanoplatelets via the reduction of exfoliated graphite oxide in the presence of poly (sodium 4-styrenesulfonate). *J. Mater. Chem*. **2006**, *16*, 155–158.

21. Stankovich, S.; Piner, R. D.; Nguyen, S. T.; Ruoff, R. S., Synthesis and exfoliation of isocyanate-treated graphene oxide nanoplatelets. *Carbon* **2006**, *44*, 3342–3347.

22. Park, S.; An, J.; Jung, I.; Piner, R. D.; An, S. J.; Li, X.; Velamakanni, A.; Ruoff, R. S., Colloidal Suspensions of Highly Reduced Graphene Oxide in a Wide Variety of Organic Solvents. *Nano Lett*. **2009**, *9*, 1593–1597

23. Cai, M.; Glover, A.J.; Wallin, T.J.; Kranbuel, D.E.; Schniepp, H.C.; Direct Measurement of the Interfacial Attractions between Functionalized Graphene and Polymers in Nanocomposites. *In Prepartion.* **2010**

24. Amnaya, P.A.; Lagoudas, D.C.; Hammerand, D.C.. Modeling of graphene-polymer interfacial mechanical behavior using molecular dynamics. *Moddelling Simul. Mater. Sci. Eng.* **2009** 17, 1-37

25. Haraguchi, K.; Farnworth, R.; Ohbayashi, A.; Takehisa, T. Compositional Effects on Mechanical Properties of Nanocomposite Hydrogels Composed of Poly (N,N-dimethylacrylamide) and Clay *Macromolecules*, **2003**, *36* (15), 5732–5741.

26. Measuring and Understanding Tg (Glass Transition Temperature) *Arlon Application Notes*. 1-4.